

PETROLOGY AND GEOCHEMISTRY
OF SOME ARCHEAN VOLCANICS,
DOME TOWNSHIP,
CENTRAL RED LAKE AREA, ONTARIO

Petrology and Geochemistry
of Some Archean Volcanics
Dome Township,
Central Red Lake Area, Ontario

by

Susan M. Cunningham

A Research Paper
Submitted to the Department of Geology
in Partial Fulfillment of the Require-
ments for the Degree
Bachelor of Arts

McMaster University

April, 1979

Bachelor of Arts (1978)
(Geology)

McMaster University
Hamilton, Ontario

Title: Petrology and Geochemistry of Some Archean Volcanics,
Dome Township, Central Red Lake Area, Ontario

Author: Susan M. Cunningham

Supervisor: Dr. B. McNutt

Number of Pages: viii, 87

Scope and Contents:

A petrological and geochemical study has been carried out on some Archean mafic and felsic volcanics of Dome Township, Central Red Lake area, Ontario. Included are a discussion on petrographic descriptions along with chemical investigations of the rocks and a discussion concerning the general problem of petrogenesis. Analytical methods used are explained, and discussions of the results are included.

Acknowledgements

The author wishes to thank the Ontario Geological Survey for allowing the collection of the field data and samples during the 1978 field season as well as for providing some of the chemical analyses and thin sections. I am grateful to Mr. J. Pirie of the O.G.S. who suggested the topic and provided advice both in the field and during the writing of this thesis. Appreciation is also extended to Mr. D. Thomson of Queen's University and Mr. G. Caldwell of the University of Windsor who aided the author in the sampling and mapping of the area.

I am grateful to Dr. R.H. McNutt; who supervised the writing of this thesis.

The author also wishes to thank Mr. L.J. Zwicker for preparation of thin sections; Mr. J. Whorwood for preparation of photomicrographs; and Mr. O. Mudroch for his assistance in the chemical analysis of the rocks. Special thanks go to Mr. D. Rees for his valuable assistance in the drafting of the figures and Miss R. Genovese who was kind enough to type the manuscript. Thanks also go to Pat Cowan of McMaster University who provided additional data from the field area.

Finally I would like to thank the graduating geology students of "79" as well as the other graduate and undergraduates, for their advice, encouragement, assistance and comic relief throughout the year.

Table of Contents

	PAGE
Scope and Contents -----	ii
Acknowledgements -----	iii
Table of Contents -----	iv
List of Tables-----	vi
List of Figures -----	vii
 Chapter	
I Introduction -----	1
1.Location and Accessibility -----	1
2.Previous Work -----	1
3.Statement of Problem -----	3
4.General Geology -----	4
5.Structural Geology -----	5
II Petrography -----	10
Description of Rock Units	
1.Komatiites -----	10
2.Mafic Volcanics -----	16
3.Intermediate Volcanics -----	18
4.Felsic Volcanics -----	20
5.Chemical Metasediments -----	28
6.Clastic Metasediments -----	28
7.Intrusive Rocks -----	30
a) Metagabbro -----	30
b) Quartz Porphyry -----	30
c) Serpentinite -----	32

	PAGE
8. Carbonatized Mafic Volcanics -----	32
III Classification of Volcanic Rocks -----	34
IV Geochemistry -----	45
1. Introduction -----	45
2. Major Elements -----	45
3. Trace Elements -----	54
V Petrogenesis -----	61
Tectonic Environment -----	62
The Tholeiitic Basalt Calc-alkali Andesite	
Problem -----	66
Genesis of the Basaltic Komatiites and	
Tholeiitic Basalts -----	69
The Felsic-Mafic Volcanic Relationship -----	70
VI Summary and Conclusions -----	71
Appendix	
Appendix A Rock Samples and Their Names -----	74
Appendix B Modal Analyses -----	76
Appendix C Accuracy of XRF Determinations -----	78
Appendix D Whole Rock Analyses -----	81
Trace Element Analyses -----	82
Appendix E Equivalent Cation Normes -----	83
References -----	85

List of Tables

Table	PAGE
I Regional Formations -----	6
II Volcanic Rock Classification -----	40
III Chemical Criteria for Komatiites-----	43
IV Chemical Variations of Volcanic Rocks -----	46
V Trace Element Variation of Volcanic Rocks -----	55
B-1 Modal Analyses -----	76
D-1 Whole Rock Analysis -----	81
D-2 Trace Element Analyses -----	82
E-1 Equivalent Cation Norms -----	83

List of Figures

Figure		PAGE
1	Location Map-----	2
2	Gravity Profile of the Red Lake Area-----	8
3	Photomicrograph of "pseudo-spinifex" texture-----	11
4	Photomicrograph of primary spinifex texture-----	11
5	Photomicrograph of primary spinifex texture-----	13
6	Photomicrograph of micro spinifex texture-----	14
7	Photomicrograph of polygonal quartz-----	14
8	Photomicrograph of microspinifex texture-----	15
9	Variolitic pillowed basalt-----	17
10	Coalesced varioles in pillow basalt-----	17
11	Photomicrograph of variolitic basalt -----	19
12	Photomicrograph of altering plagioclase phenocrysts-----	21
13	Photomicrograph of altering plagioclase phenocrysts-----	21
14	Photomicrograph of granophyric intergrowth-----	23
15	Slurry structures in the lapilli-tuff-----	23
16	Photomicrograph of fractured quartz-----	24
17	Photomicrograph of "broken" quartz-----	24
18	Photomicrograph of undulose extinction in quartz-----	25
19	Graded bedding in the lapilli-tuff -----	25
20	Bedding and folding in the ash tuff-----	26
21	Green chromite patch in the ash tuff-----	26
22	Photomicrograph of lapilli-tuff-----	27
23	Folded lean iron formation-----	29

Figure	PAGE
24	Photomicrograph of serpentinite ----- 29
25	Photomicrograph of "turkey-track" gabbro ----- 31
26	Photomicrograph of extensive carbonitization ----- 33
27	$\text{Na}_2\text{O} + \text{K}_2\text{O}$ vs SiO_2 Diagram ----- 36
28	AFM Diagram ----- 37
29	Jenson Cation Plot ----- 38
30	Normative C.I. vs Normative Plagioclase Composition ----- 39
31	Ternary Diagram of An-Ab-Or----- 41
32	TiO_2 vs MgO Diagram ----- 48
33	TiO_2 vs SiO_2 Diagram ----- 49
34	TiO_2 vs Al_2O_3 Diagram ----- 51
35	Al_2O_3 vs $\text{FeO}/(\text{FeO} + \text{MgO})$ Diagram ----- 52
36	Rb vs K Diagram ----- 56
37	Cr vs Ni Diagram ----- 60
38	Ti/100 - Zr - Yx3 Ternary Diagram ----- 63
39	Ti/100 - Zr - Sr/2 Ternary Diagram ----- 64
40	Ti vs Zr Diagram ----- 65
41	Zr vs MgO Diagram ----- 68

Chapter 1 Introduction

1. Location and Accessibility

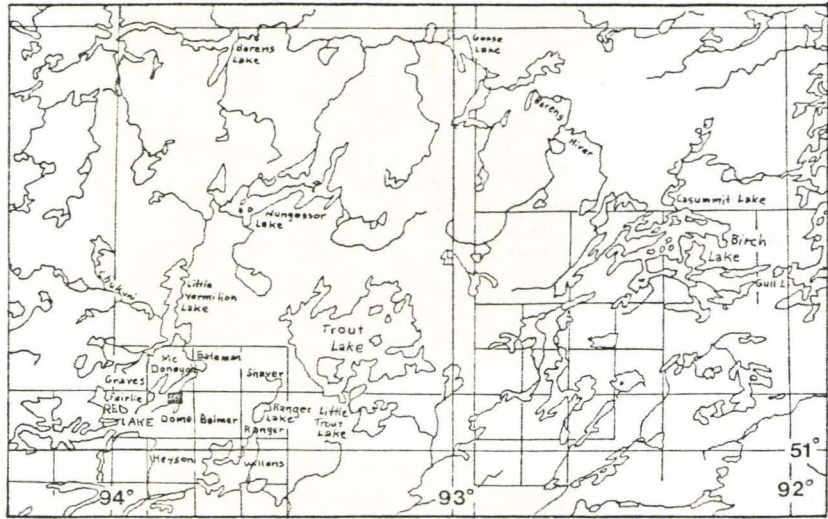
The map area is in the north-central portion of Dome Township, located in the central Red Lake area, bounded by latitudes $51^{\circ}03'47''$ and $51^{\circ}05'08''$ N and longitudes $93^{\circ}40'56''$ and $93^{\circ}43'21''$ W. It is within the Red Lake Archean metavolcanic-sedimentary belt in north-western Ontario in the Patricia Portion of the District of Kenora. It can be located on Map 2074, Dome Township, Kenora District, O.D.M., NTS reference 52N/4, 1965; and the location map (Figure 1).

The map area is approximately 2 km by boat, north of the town of Cochenour and 15 km by road from Red Lake via highway 125. The long axis of the map area trends E-W for 3 km and the short axis for 2.5 km. It consists of 14 small islands and the NE shore of McKenzie Island.

2. Previous Work

Robert Bell of the Geological Survey of Canada (G.S.C.) first visited the Red Lake area in 1883, when he noted the presence of what he termed some interesting minerals in the Huronian Rocks. The area was then examined geologically for the first time in 1893 by D.D. Dowling of the G.S.C. during the course of an exploration from the English to the Berens River. The first recorded discovery of gold was made in 1897 by a prospecting venture headed by R.J. Gilbert of the Northwestern Ontario Exploration Company. In 1922 a party of prospectors became interested in the area, discovered a vein containing quartz and argentiferous galena and some small gold-bearing quartz stringers, sparking off increased activity in the area.

Fig. 1 - Location Map of the study area. Scale: 1:1,584,000 (From Pirie, 1977)



E.L. Bruce (1924) of the Ontario Division of Mines (O.D.M.) examined the area and stated that further prospecting appeared to be warranted. The interest sparked by E.L. Bruce resulted in re-examination by J.E. Hawley and E.L. Bruce in the summer of 1926. The results of exploration were disappointing and interest in the area decreased. However, in 1933 with an increase in the price of gold, interest picked up again at which time M.E. Hurst surveyed the mineral occurrences. This was followed by mapping and a report by H.C. Horwood (1940).

Dome Township was first mapped in considerable detail by Horwood (1940) and later by S.A. Ferguson (1961). Due to continued interest in gold, the area is presently being remapped by J. Pirie of the Ontario Geological Survey (O.G.S., formerly the O.D.M.).

3. Statement of Problem

In western Bateman Township, N.E. of Dome Township, a sequence of rocks trending N.E. form the west limb of a major anticline with steeply dipping bedding and foliation. In Balmer Township, directly east of Dome Township, the same sequence trend in a rough east-southeast direction. The location of change of these two trends occurs mainly in Dome Township (Pirie, 1977). However, the exact relationship between the trends is not known.

Farther south along strike of the northeast trending mafic volcanics, felsic volcanics are found to interfinger with the mafic, perhaps indicating a facies change. Both rock sequences are then overlain by a mafic sequence to the north, along the same strike.

In the summer of 1977, while employed by O.G.S. under the supervision of J. Pirie, the author spent approximately a week and a half investigating

the study area. The purpose of the project was to produce a detailed map and collect samples for lab chemical studies in an effort to understand the relationships between the felsic and mafic volcanics and the variable trending rock sequence.

Due to good exposure along the shoreline of the islands, most of the detailed work was completed via canoe. Roughly 150 samples were initially collected for mapping purposes. Of these, 26 samples were selected for chemical and thin section analysis. Supplemental information was obtained through the analysis of 9 additional thin sections and 2 chemical analysis provided by J. Pirie, and 10 thin sections and/or chemical analysis provided by Pat Cowan of McMaster University.

4. General Geology

The Red Lake area consists of Archean volcanic and sedimentary rocks, later intruded by various felsic stocks. In Dome Township, these intrusions are in the form of the Dome and smaller McKenzie Island Stocks (Ferguson, 1966). Northeasterly trending mafic meta-volcanics of Dome and McDonough Townships meet east-southeasterly trending metavolcanics of Dome and Balmer Townships around the northerly tip of McKenzie Island and south of East Bay of Bateman Township. Their relationship has presently not been confirmed. The lower part of the northeasterly metavolcanics which run into the study area, consist of massive and variolitic pillowed volcanic flows. Interbedded with the flows are minor metasediments including cherty, magnetite-bearing iron formation and reworked clastic mafic debris. The east-to southeasterly trending mafic metavolcanics are interbedded with magnetite and pynhotite-bearing iron formation and minor chert (Pirie, 1977).

No felsic stocks are found within the study area, but minor intrusions are found predating deformation and metamorphism. Some of these intrusions are the subvolcanic equivalents of the mafic volcanics (Pirie, 1977). The geological succession of the Red Lake area may be seen in Table I. Rock units found within the study area are indicated with a star.

5. Structural Geology

A gravity profile of the Red Lake Area was determined by F.S. Grant (see Ferguson, 1966) and is reproduced in Figure 2. He considered the greenstone belt to be an asymmetrical synclinorium, 40 km. in length, 7.5 km deep, containing a central lighter core to a depth of 2.2 km. assumed to consist of acidic, sedimentary or granitic rocks.

Locally, within the study area, pillow structures in the mafic metavolcanics and graded bedding of the felsic (pyroclastic) metavolcanics indicate a younging direction to the northwest. Foliation swings from a northeasterly orientation in the northern islands to a southeasterly orientation on the northern tip of McKenzie Island. Both bedding and foliation dip steeply varying slightly from east to west throughout most of the area. The exception to this rule occurs on McKenzie Island where the dips shallow to 70° S.W. most likely due to the intrusion of the McKenzie Island Stock which dips 70° W according to Ferguson (1966). Tight isoclinal folds were observed on the north shore of the most westerly island of the area within the pyroclastics, the fold axis trending parallel to the foliation. The general plunge direction is considered to be southwards (Pirie, personal communication, 1979) (Ferguson, 1966).

Table 1 Regional Formations (Kita, 1978)

Phanerozoic

Cenozoic

Quaternary

Pleistocene and Recent

Glacial till, sand, gravel, varved clay, silt and
organic mud

-UNCONFORMITY-

PRECAMBRIAN

EARLY PRECAMBRIAN

METAMORPHOSED INTERMEDIATE TO FELSIC INTRUSIVE ROCKS

PLUTONIC BATHOLITHIC PHASES

granodiorite, trondhjemite, syenodiorite, leucotondhjemite,
aplite, gabbro, amphibolite, pegmatite, diorite gneiss

-INTRUSIVE CONTACT -

HYPERBYSSAL PHASES

trondhjemite, *quartz porphyry, feldspar porphyry, quartz-feldspar
porphyry, felsite, biotite granodiorite

-INTRUSIVE CONTACT-

METAMORPHOSED MAFIC TO ULTRAMAFIC INTRUSIVE ROCKS

gabbro, leucogabbro, diorite, peridotite, *serpentinite, pyroxenite,
lamprophyre

-INTRUSIVE CONTACT-

METAVOLCANICS AND METASEDIMENTS

METASEDIMENTS

Chemical Metasediments

* chert, *iron-formation, marble calc-silicates

Clastic Metasediments

conglomerate, arkose, arenite, *wacke, mudstone, *slate,
argillite

METAVOLCANICS

Felsic Metavolcanics

*pyroclastic breccia, tuff-breccia, *tuff, *lapilli-tuff, lapillistone

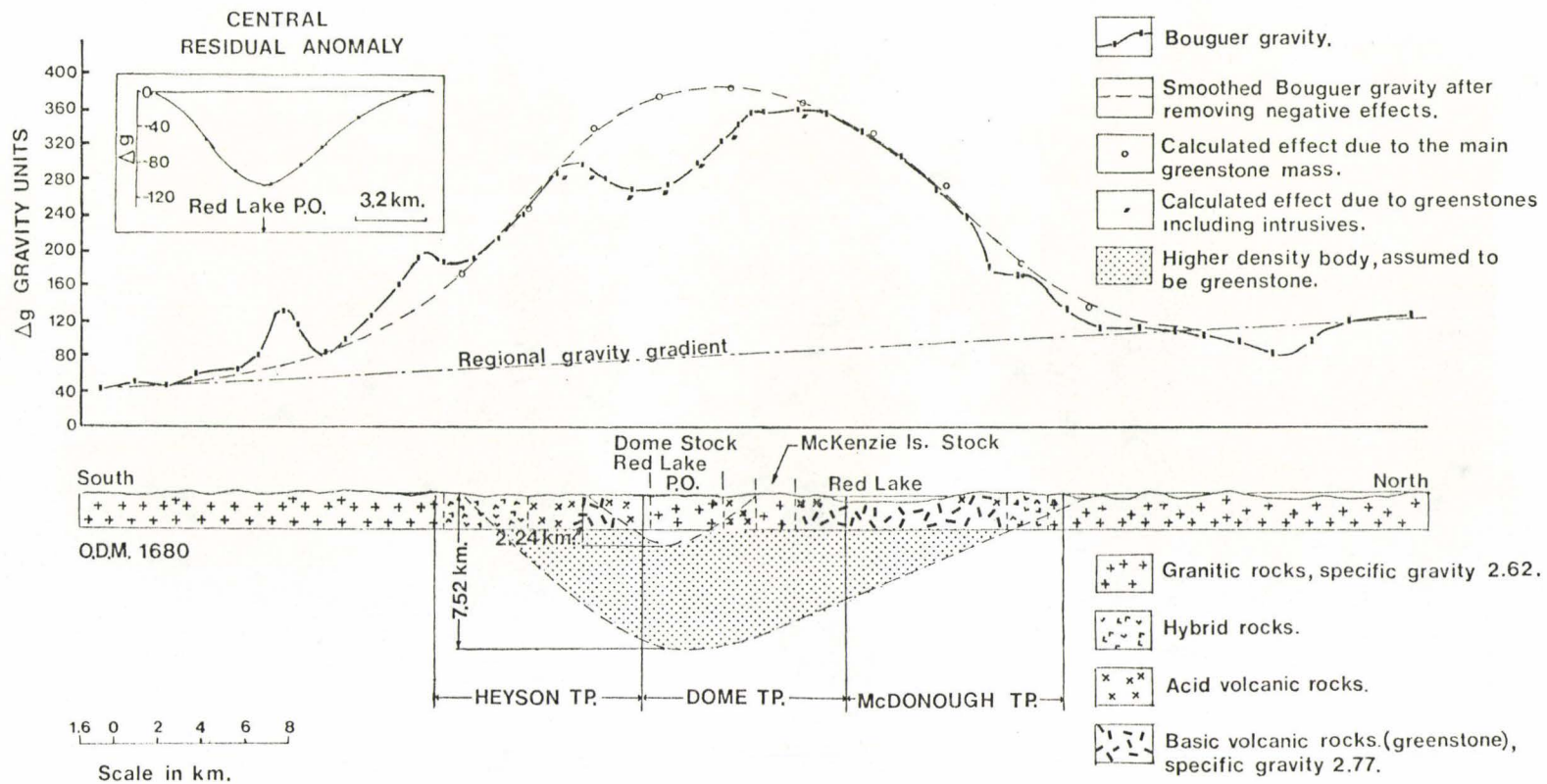
Intermediate Metavolcanics

lapilli-tuff, lapillistone, tuff-breccia, pyroclastic breccia, flow
(massive to foliated)

Mafic Metavolcanics

*massive to foliated flow, *pillowed flow, *pillow breccia, *variolitic
flow, *gabbro, tuff

Fig. 2 - North-south gravity profile, rock types exposed at surface, and cross-section of Red Lake greenstone and central core as interpreted from gravity data; assumed strike length is 32 km. After an unpublished work by F.S. Grant, with slight modifications to the geological cross-section and legend by S.A. Ferguson (from Figure 10, Ferguson, 1966).



Cherty iron formation, occasional clastic, metasediments and
variolitic lavas form marker horizons throughout the area.

Chapter II Petrography

Description of Rock Units

1. Komatiites

The northern-most lavas within the area are komatiitic, trending along the NE strike and pinching out towards the most westerly island. Minor flows are found farther south, often grading into basalt.

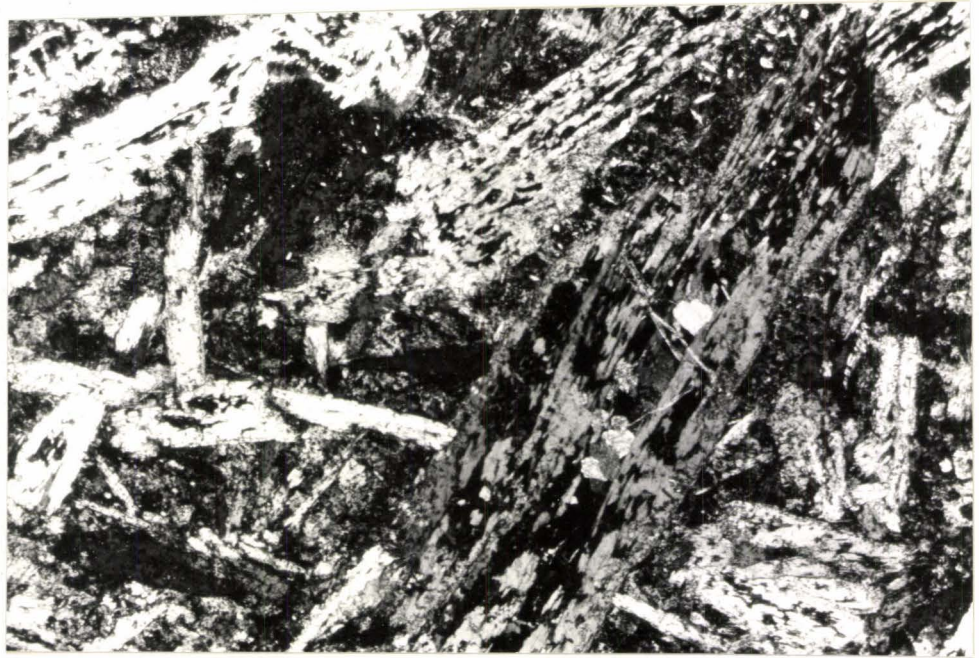
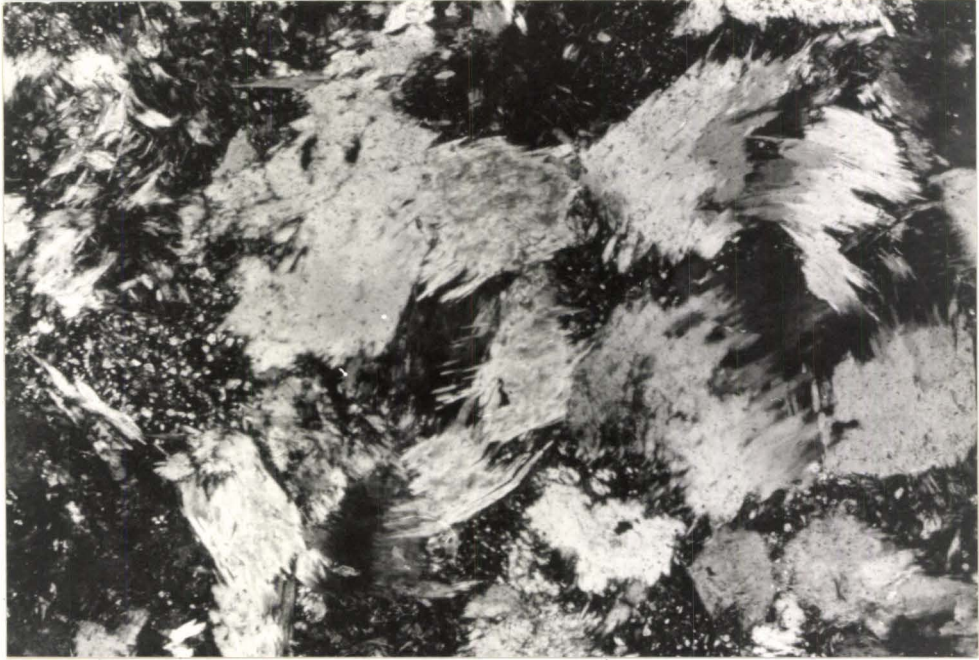
The basaltic komatiites are light to dark green in colour dominated by prismatic amphibole crystals, often exhibiting spinifex texture. Pirie (personal communication), 1979) has noted basaltic komatiites with spinifex texture farther northeast along strike with the study area, within the same sequence of rocks.

"Blocky pillows" are located in the northeast portion of the study area along with flow-top breccias which extend farther west within the komatiitic unit. The amphibole crystals are secondary, replacing original pyroxene and vary in size from 0.5 mm to 2.5 cm parallel to the c axis.

It is thought that some of the rocks exhibit a "pseudo-spinifex" texture while others exhibit a primary spinifex. The criteria for separating the two has been based upon the relative dimensions of the amphibole crystals. "Pseudo-spinifex" exists where the amphibole crystals are of an equant, stubby, prismatic to tabular form, usually bent with jagged terminations. This indicates slow growth of the original pyroxene and recrystallization of the amphibole during metamorphism (Figure 3) (Pirie, personal communication, 1979). Primary spinifex textures exist when the amphibole crystals are of a long, prismatic, needle-like form, suggesting rapid growth, in a crystal-free ultramafic liquid in situ (Pyke, et.al., 1973). The primary spinifex occurs

Fig. 3 - Photomicrograph of amphibole crystals showing "pseudo-spinifex" texture (sample 24). (Crossed Nicols).
Magnification is 63 x

Fig. 4 - Photomicrograph of skeletal amphibole crystals showing primary spinifex texture. (Sample 21 b). (Crossed Nicols)
Magnification is 25 x



in two distinct sizes, averaging 2.0 cm and 0.3 mm in length. They have a subparallel to radiating arrangement on a large scale, easily recognized in hand specimen (Figure 5). Arndt et. al. (1977), discussing the Munro high MgO basaltic komatiites (MgO > 10%) mention clinopyroxene spinifex texture in flow tops which grade downwards into microscopic spinifex texture in which the clinopyroxene needles are randomly oriented. Their microscopic spinifex texture is composed of clinopyroxene needles of 0.5 to 1.0 mm in length, and the groundmass consists of devitrified glass or an intergrowth of prismatic grains of clinopyroxene and plagioclase. This appears to be the case in the basaltic komatiites in the study area, the main difference being the low Mg content (MgO < 10%) and a chlorite-sericite matrix. The basaltic komatiites in the Munro Township of low MgO content exhibited an intergrowth of clinopyroxene and plagioclase needles. The plagioclase needles are absent in the spinifex texture of the study area, but may have been altered to sericite and chlorite.

Sample 21b exhibits the large-scale primary spinifex texture, and is situated close to the flow-top breccia. The crystals are skeletal, often containing chlorite and small rounded anhedral crystals of epidote (Figure 4). Samples 200, 206 and JP294 exhibit the "micro-spinifex" texture which is not observable in hand specimen. It consists of more randomly radiating prismatic amphibole crystals (Figure 6). Alteration to chlorite is apparent, to an Fe-Mg form showing anomalous violet-to Berlin-blue interference colours (Shelley, 1975) (Figure 8). Samples 200 and JP294 contain minor polygonal quartz grains (Figure 7). A few opaque grains are scattered throughout the slides in a random fashion.

Fig. 5 - Photomicrograph of the basaltic komatiites of the study area.

Primary spinifex texture of the amphibole crystals is evidenced.

(Sample 21b) (Crossed Nicols)

Magnification is 6 x



Fig. 6 - Photomicrograph of amphibole crystals showing microspinifex texture, altering to an Fe-Mg chlorite. (Sample 76) (Crossed Nicols)

Magnification is 25 x

Fig. 7 - Photomicrograph of polygonal quartz showing strained extinction and fragturring due to deformation (Sample 106) (Crossed Nicols)

Magnification is 63 x

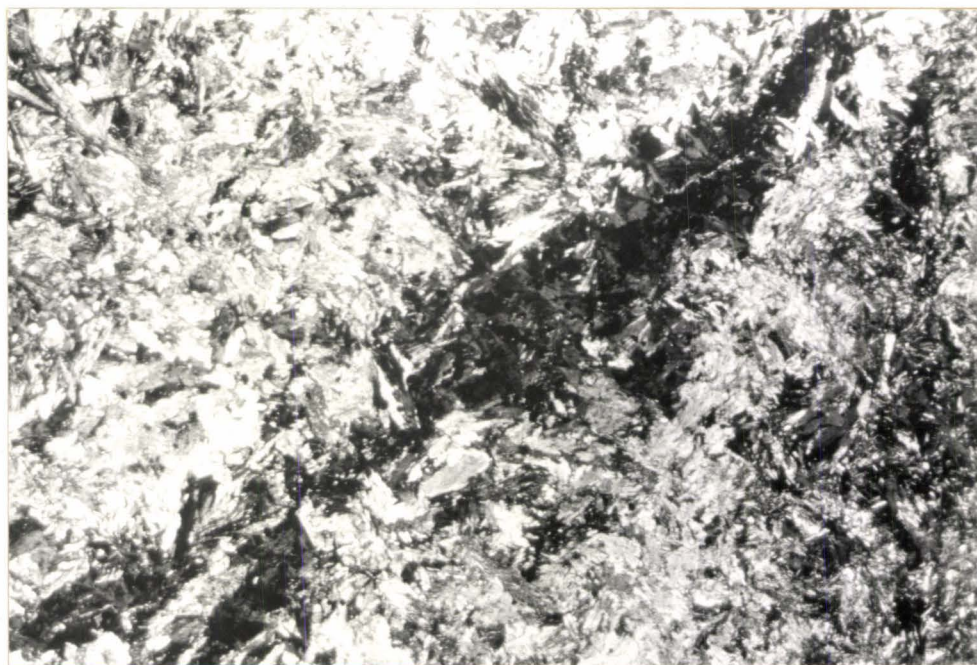


Fig. 8 - Photomicrograph of basaltic komatiite showing micro spinifex

(Sample 76) (Crossed Nicols)

Magnification is 6 x



2. Mafic Volcanics

Mafic volcanics predominate in the western islands pinching and interfingering with more intermediate volcanics. It has been suggested (Pirie, personal communication, 1979) that the intermediate volcanics are in fact altered basalts. This question will be dealt with later. In this chapter the mafic and intermediate volcanics will be dealt with separately.

The mafic volcanics are a dark green, aphanitic, massive to pillowed, variolitic to "non-variolitic" unit. The pillows are elongated parallel to foliation and average dimensions of 14 cm by 8 cm (Figure 9).

The variolites tend to be concentrated near the rim of the pillows, but in some localities are found coalesced within the centres. They are white on the weathered surface and a lighter green than the dominant mafic material on the fresh surface (Figure 10).

Thin section analysis reveals a predominance of chlorite, calcite and sericite in the varioles, which tend to be elongated parallel to the foliation (Figure 13). A rim of chlorite often surrounds the varioles which in turn are surrounded by the pillow matrix. This consists of subhedral to euhedral altered amphibole and olivine phenocrysts in a calcite-chlorite-matrix. Under plain light colourless prismatic to tabular crystals are observed possibly indicating the presence of original feldspar which has been extensively altered to sericite and chlorite. Pirie (personal communication, 1979) has noted the presence of variolitic basalts farther NE along strike, in which amphibole is the dominant mineral within the varioles. Thus it is felt that the varioles may have originally had a mafic composition. Analysis of varioles collected by Pirie (1979) at sample location JP488 however, indicated a highly felsic content. For full analysis see Appendix D.

Fig. 9 - Variolitic pillowed basalt located at sample site 400.

Fig. 10 - Coalesced varioles in the pillow basalt located at sample site
108 (JP 488)



Thus it appears that varioles of contrasting mafic and felsic composition exist within a reasonably close proximity of the area.

In Munro Township, Arndt et. al. (1977) noted the presence of tholeiitic volcanic rocks of basaltic to andesitic composition alternating with the slightly thinner successions of komatiitic lavas in a concordant manner. The komatiites were pillowed or massive with brecciated flow-topes. The basaltic lavas were fine-grained and equigranular, and contained phenocrysts of clinopyroxene or more rarely plagioclase. Olivine was absent.

The main difference between the tholeiitic flows of Munro Township and the mafic volcanics of the study area is the presence of varioles and minor olivine within the pillows of the latter. In both areas, the effects of regional metamorphism were more conspicuous in the tholeiites than in the basaltic komatiites where the plagioclase and pyroxene are being replaced by sericite and calcite.

Opaques are associated with the chlorite in the pillow matrix of the study area, and scattered throughout the slide. Magnetite was noted in some instances to form a stylolite-like fabric within the dominantly chlorite matrix.

3. Intermediate Volcanics

Dominantly massive, aphanitic, grey to grey-green intermediate volcanics are located within the central to southern portion of the study area, closely associated with the mafic volcanics. Pillows are found in a few localities.

Again, as noted in the section under mafic volcanics, volcanic rocks of andesitic composition were noted with the tholeiitic basalts of Munro Township (Arndt et. al., 1977).

Fig. 11 - Photomicrograph of variolitic basalt. Olivine crystals are located in the matrix surrounding the varioles. (Sample JP 290) (Crossed Nicols)

Magnification is 6 x



Microscopic examination revealed plagioclase phenocrysts occurring as cloudy, tabular laths, occasionally zoned, and altered to sericite (Figure 12, 13). However, the Michele-Levy Test was still possible to use and gave a composition of An_{40} - An_{48} . The phenocrysts measure up to 1.0 mm in length and average 0.5 mm. Alkali-feldspar and quartz are often present in minor amounts as euhedral crystals in the matrix. The quartz may exhibit a biaxial flash-figure due to metamorphism. It occasionally shows embayments and inclusions of glass. A pilotaxitic matrix of sericite and chlorite has completely replaced any original microlites if they did indeed, exist.

Sample 209 contains small, tabular, highly pleochroic brown biotite averaging a grain size of 0.6 mm. Secondary epidote crystals with corroded rims are located at sample sites 140 and 166 in minor amounts varying from euhedral hexagons and tabular laths to anhedral form. Carlsbad twinning is present in a few cases. Magnetite grains are scattered throughout.

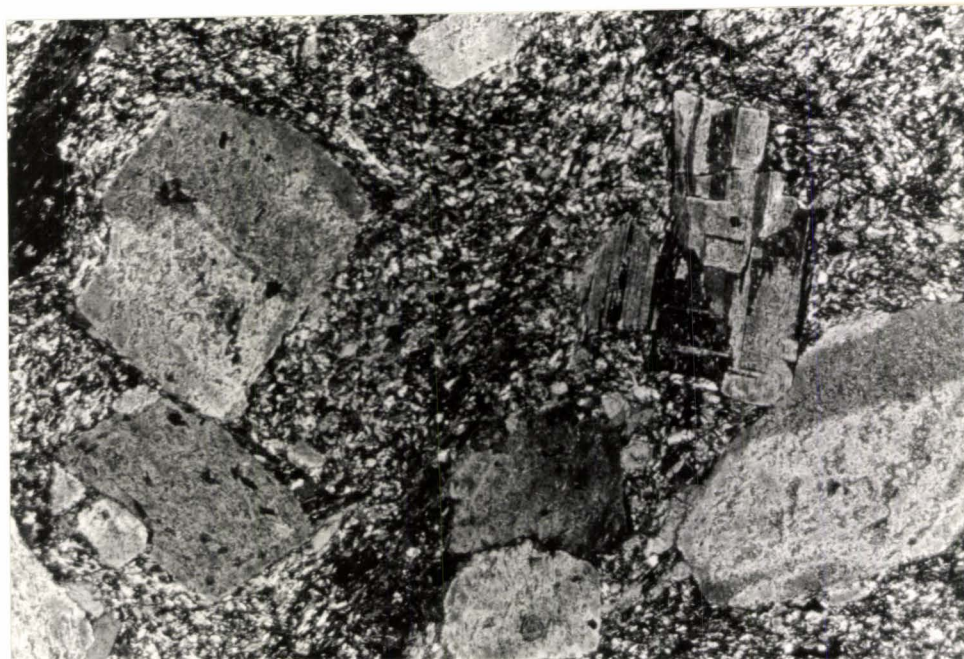
4. Felsic Volcanics

Felsic rocks in the form of pyroclastics are found in the western portion of the study area. Volcanic breccia is located on the NW shore of McKenzie Island, with the blocks ranging up to 15 cm. in the greatest dimension. A trend towards smaller fragments exists in the northwesterly direction. The central-western islands contain a dominantly matrix-supported lapilli tuff grading into an ash tuff on the most NW island.

The volcanic breccia is dominated by blocks of quartz porphyry containing quartz eyes within a felsic matrix. The blocks are elongate parallel to foliation. Thin section analysis reveals the presence of

Fig. 12 - Photomicrograph of altering plagioclase phenocrysts. (Sample
166) (Crossed Nicols)
Magnification is 63 x

Fig. 13 - Photomicrograph of altering plagioclase phenocrysts showing slight
zoning (Sample 106) (Crossed Nicols)
Magnification is 63 x



angular quartz phenocrysts, rectangular to tabular laths of plagioclase with fine lamellae in albite twinning, all altering to sericite. Rock fragments are present varying in composition from quartz porphyry, plagioclase porphyry to biotite, magnetite, sphene, epidote and calcite aggregates. Granophyric intergrowth phenocrysts of quartz and feldspar are sparsely scattered (Figure 14).

In hand specimen the lapilli tuff is dominated by quartz-eye lenses oriented parallel to foliation. Graded bedding and slump structures are evident (Figure 15). Minor mafic and pumice fragments (Pirie, personal communication, 1978) up to 2 cm in diameter are found throughout. They also show slight elongation parallel to foliation. Bedding is oriented at an acute angle to the foliation ($2-4^\circ$ against foliation trends of $70-90^\circ$).

Mafic rock fragments tend to be more abundant, often containing amphibole or biotite crystals. Phenocrysts vary from angular quartz, often broken and corroded (Figures 16, 17, 18) to 0.2 mm broken, frequently zoned, altered plagioclase with polysynthetic twinning to amphibole; all in a chlorite-muscovite-sericite matrix. Pressure shadows, deformed twinning and evidence of rotation of quartz crystals are evidence of deformation during metamorphism.

Beds of tuff vary in thickness from 7 mm to several meters, often showing graded bedding (Figure 19) and slump structures. Small tight isoclinal folds were noted in some localities, their fold axis trending parallel to foliation (Figure 20). Patches of chrome-rich green mica were noted in the field as an irregular occurrence (Figure 21).

Angular quartz crystals again are characteristic in thin section,

Fig. 14 - Photomicrograph of granophynic intergrowth phenocryst of quartz
and feldspar (Sample 297) (Crossed Nicols)
Magnification is 63 x

Fig. 15 - Slump structure in the lapilli tuff located at sample site 135.

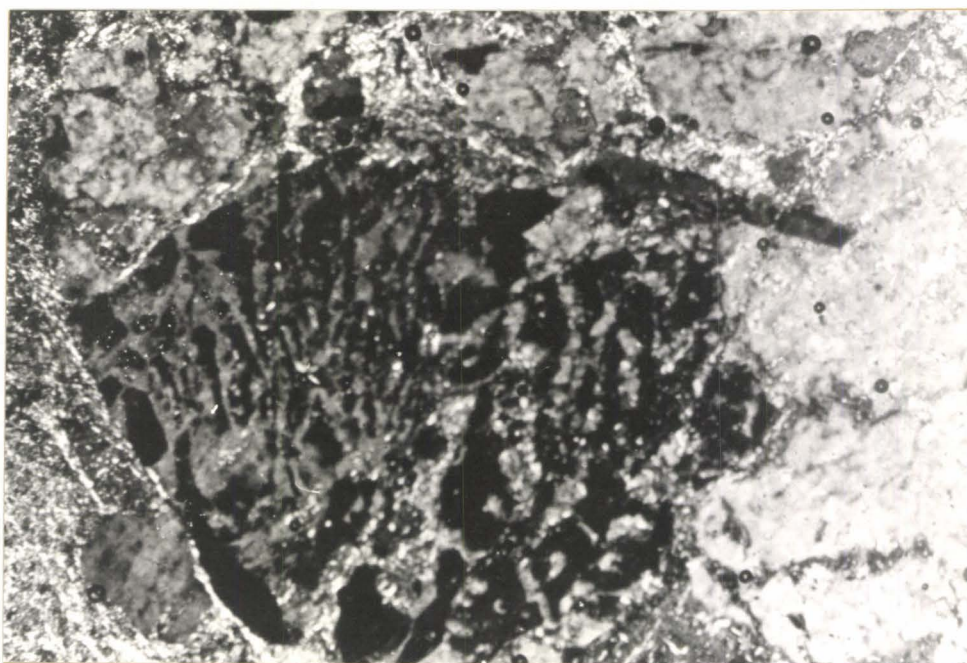


Fig. 16 - Photomicrograph of fractured quartz-"eye" in the lapilli tuff.

(Sample JP 299) (Crossed Nicols)

Magnification is 25 x

Fig. 17 - Photomicrograph of a quartz "eye" split in two by deformation.

(Sample 135) (Crossed Nicols)

Magnification is 63 x

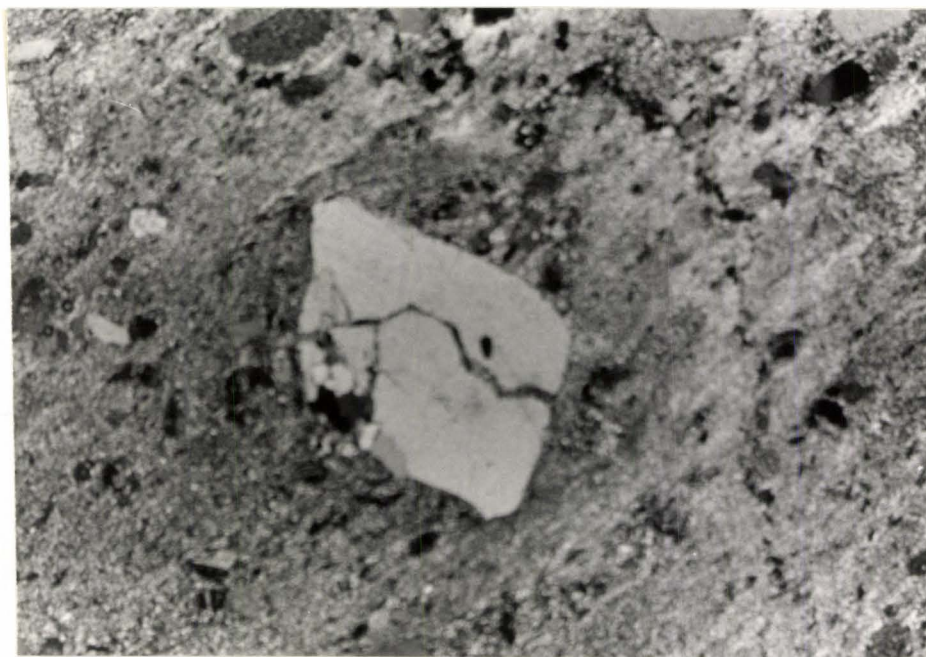
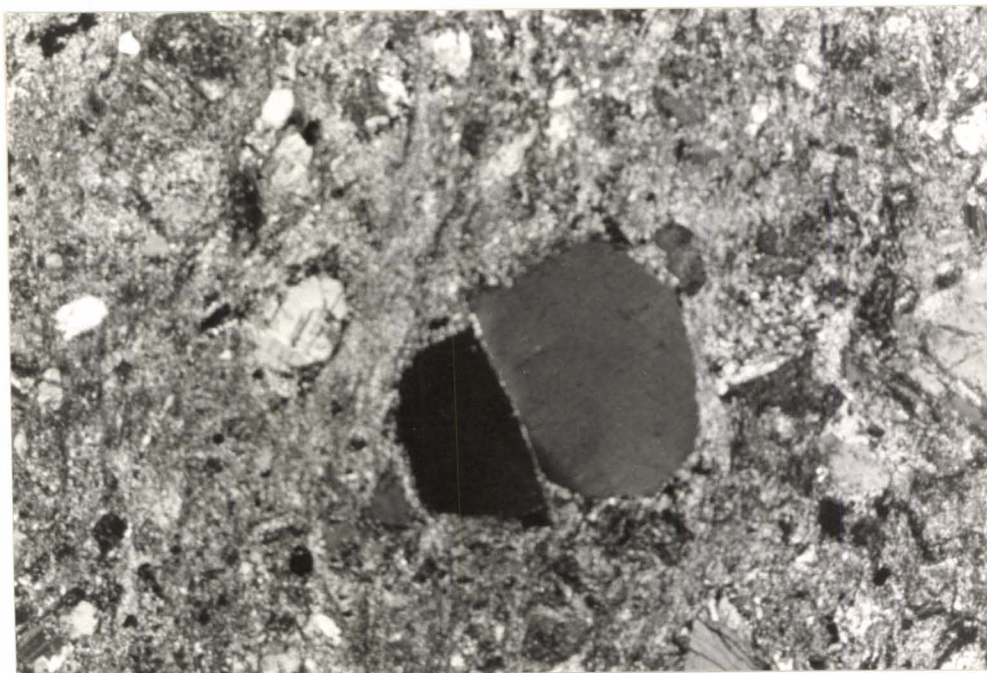


Fig. 18 - Photomicrograph of an angular quartz crystal showing undulose extinction (Sample 136) (Crossed Nicols)
Magnification is 25 x

Fig. 19 - Graded bedding in the lapilli-tuff located at sample site 135.

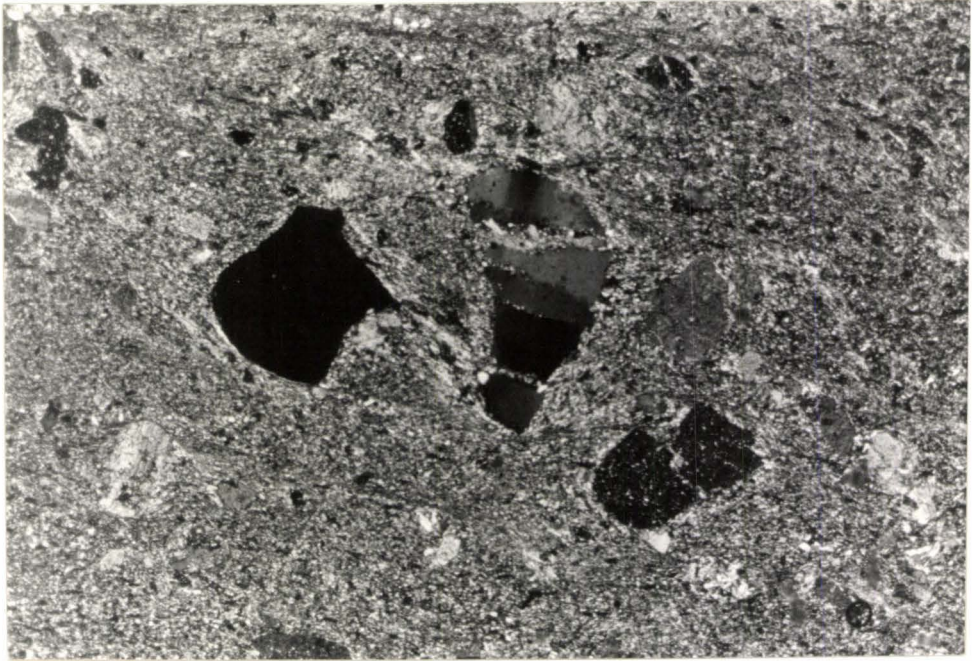


Fig. 20 - Bedding and folding in the ash tuff located at sample site 160.

Fig. 21 - Green chrome-rich patch in the ash tuff located at sample site 150.

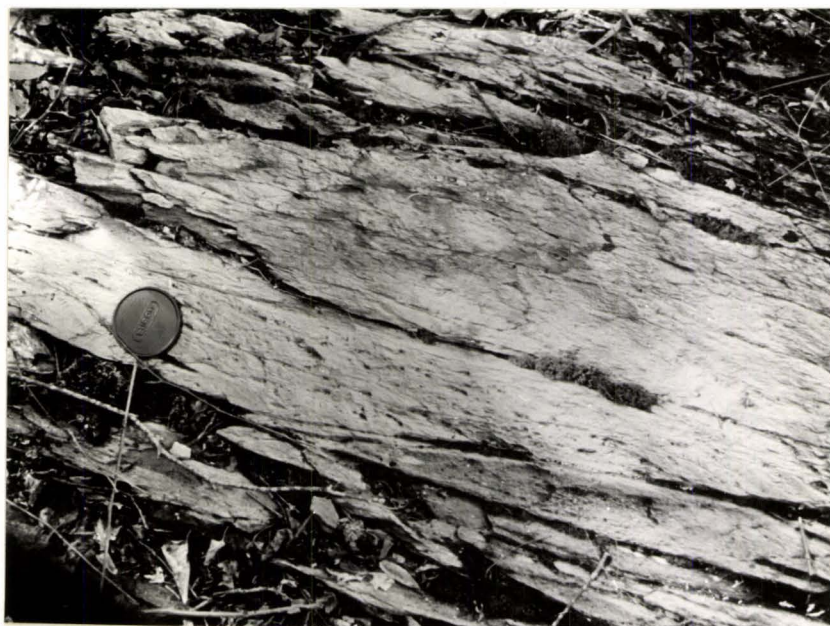
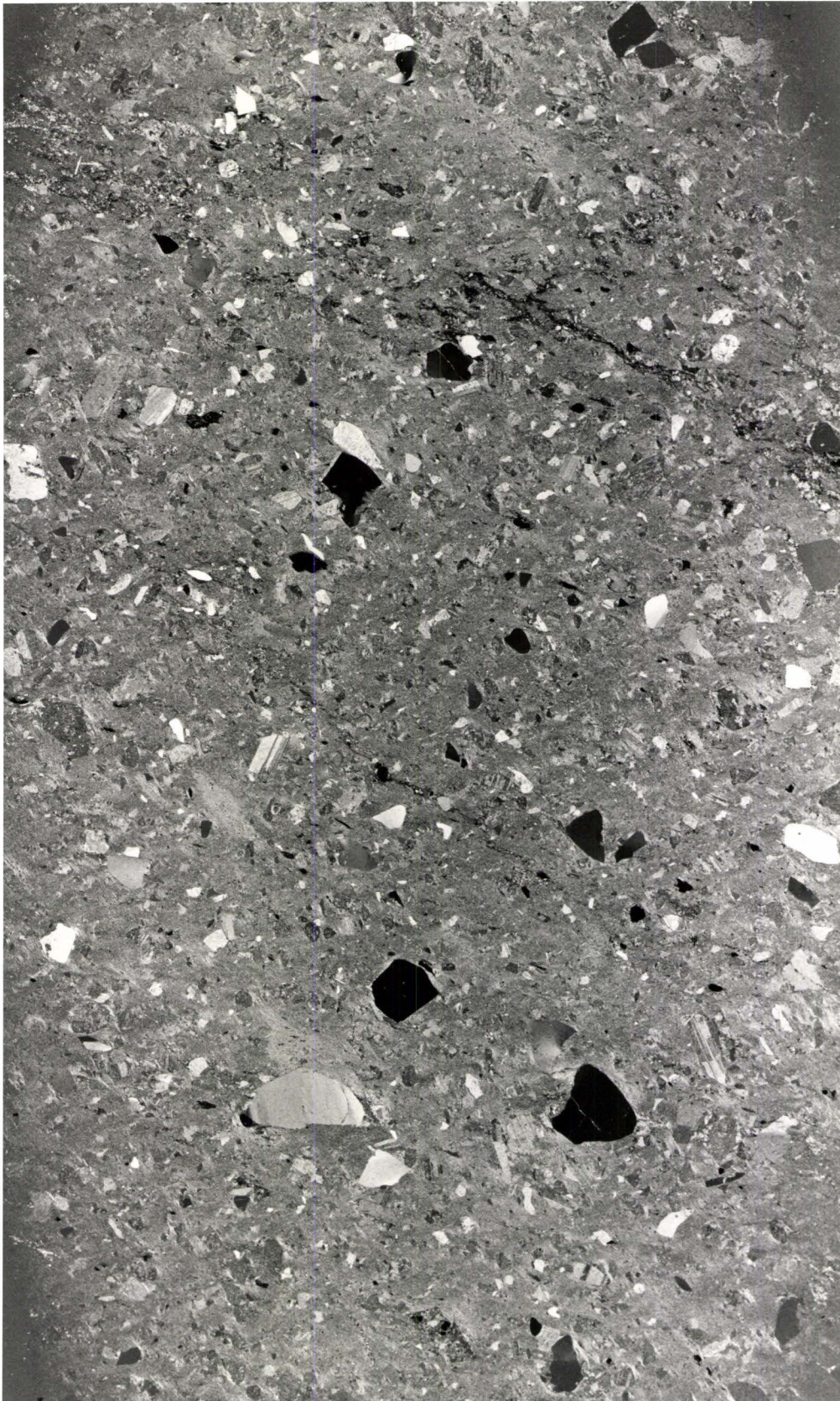


Fig. 22 - Photomicrograph of angular quartz "eye" phenocrysts and surrounding matrix in the lapilli-tuff (sample JP 485) (Crossed Nicols)
Magnification is 6 x



as are rectangular phenocrysts of plagioclase averaging a composition of An₃₇. Alkali-feldspar is also present showing microcline twinning, as is biotite which is usually closely associated with chlorite. Characteristic sericite, muscovite and chlorite constitute the fine-grained fibrous matrix.

5. Chemical Metasediments

Chemical metasediments located throughout the study area are good marker horizons. Lean Iron-formation consists of alternating bands of chert and magnetite (Figure 23), the chert varying in colour from buff white to dark grey and containing thin beds or laminae (sample 99); or reworked clastic mafic debris in clasts up to 4 X 2 cm. Magnetic readings are variable (samples PC107 to 110).

Spotty reddish-brown rust coloured stains due to weathering are indicative of oxidation of sulfides.

An aeromagnetic survey of the Red Lake area was carried out by the O.G.S. (Preliminary Map B 1572, 1978) on which the iron formation shows up as a positive anomaly. The various beds are not persistent over long distances along strike and tend to be narrow bands only a few feet in thickness.

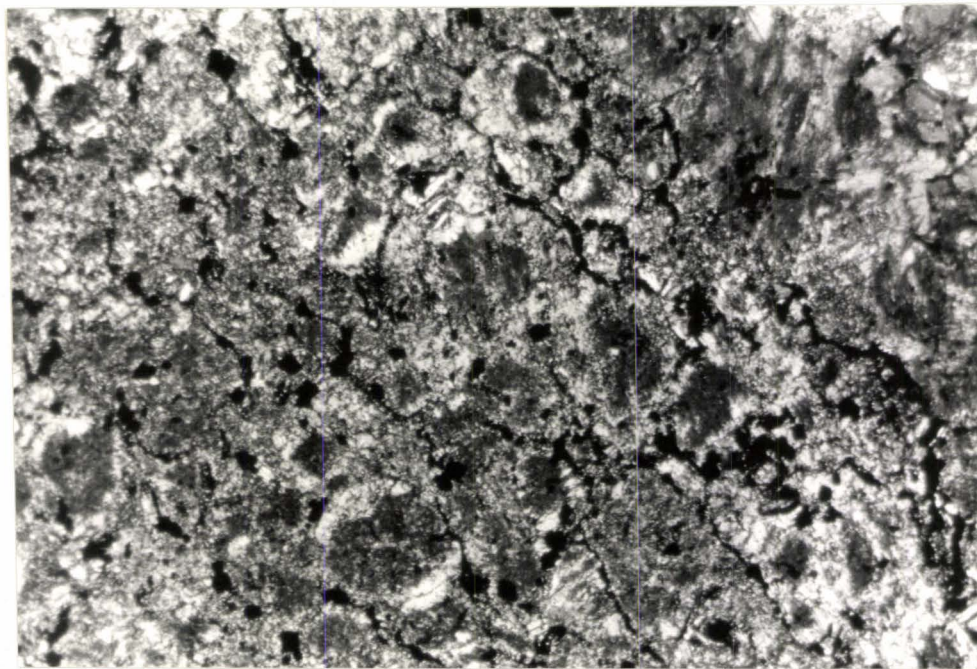
A narrow band of limestone was located on the most NW island of the area trending parallel to the foliation. West of the area limestones have been observed by Ferguson (1966) and Pirie (personal communication, 1978).

6. Clastic Metasediments

Clastic metasediments are a very minor constituent in the study area and are found associated with iron-formations and volcanics on the NW shore of McKenzie Island and the most northwesterly island. Just to the west

Fig. 23 - Folded lean iron-formation located at sample site 207

Fig. 24 - Photomicrograph of serpentinite. Note the magnetic outlining
the original olivine crystal shape (Sample 73) (Crossed Nicols)
Magnification is 25 x



of the study area the felsic volcanics pinch out and the clastic metasediments predominate. They consist of wackes and mudstones, individual beds ranging in thickness from a few feet to several yards. Secondary calcite is abundant.

7. Intrusive Rocks

a) Metagabbro

Two intrusive dykes of metagabbro, several yards in width are located in the most south-westerly island. The dykes trend 120° and 73° . Ferguson (1966) notes that in Dome Township some of these rocks are most likely the coarser-grained parts of flows whereas others are intrusive sills and dykes. He considers them to be of several ages and associated with the basalts and felsic volcanics.

They consist of plagioclase phenocrysts up to 4 mm in length in a fine-grained, dark green to black matrix. The plagioclase ranges in composition from An_{48} to An_{53} . It exhibits polysynthetic albite twinning and zoning is not infrequent. Amphibole and carbonate dominate in the matrix (Figure 25). Magnetite occurs as an accessory mineral.

b) Quartz Porphyry

Quartz porphyry intrusions are located at sample site 105 and the southeast island. Phenocrysts of quartz and feldspar (composition An_{33}) are found within a dominantly glassy matrix. There are trace amounts of amphibole and magnetite as well as the ever-present secondary calcite. The quartz that does exist in the matrix is polygonal, as are some of the phenocrysts. Rotation and compression is evident. The plagioclase is cloudy under plain light and altering to sericite.

Fig. 25 - Photomicrograph of the "turkey track" gabbro showing plagioclase phenocrysts in a predominantly amphibole and carbonate matrix (Sample 163) (Crossed Nicols)
Magnification is 6 x



c) Serpentinite

An intrusion of serpentinite is located at sample site 73. The fresh and weathered rock surface is a grey colour, green serpentine being visible on the fresh surface. The rock is extremely dense and magnetic.

The secondary nature of serpentine is evidenced in thin section where it is the alteration product of olivine. The original olivine crystal form is outlined by secondary magnetite (Figure 24). Epidote and pyrite cubes are present in trace amounts. Secondary calcite constitutes approximately 20%.

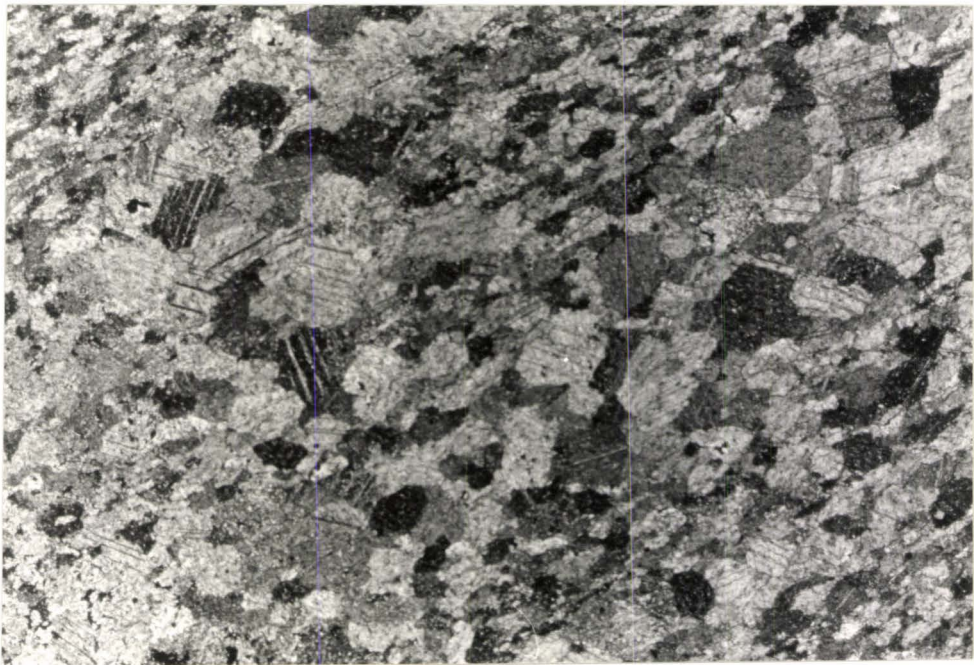
8. Carbonatized Mafic Volcanics

Carbonitization within the study area varies from virtually non-existent to extensive replacement. Extensive replacement occurs in the SE portion of the study area, where a green "carbonate" which weathers to a rust colour is located. Thin section analysis indicates almost total replacement of calcite. However, gradations of carbonitization do occur within the immediate vicinity, the "carbonate" grading into mafic volcanics. Figure 26 shows the extensive carbonate replacement of sample site 112 which both Ferguson (1966) and Horwood (1940) attribute to carbonitization.

Fig. 26 - Photomicrograph of extensive carbonitization of the mafic lavas.

(Sample 112) (Crossed Nicols)

Magnification is 25 x



Chapter III Classification of Volcanic Rocks

Due to metamorphism and the fine-grained nature of the volcanic rocks, a classification scheme based on the chemistry of the rocks must be adopted. Two such schemes have been utilized.

The first is based on the method developed by Irving and Baragar (1971). Using various chemical criteria, the volcanic rocks are divided into two major divisions, subalkaline and alkaline rocks. Further classification divides the common volcanic rocks into the tholeiitic basalt series, the alkali olivine basalt series and the calc-alkali series.

The second scheme is one proposed by Jenson (1976) for the sub-alkaline rocks. He notes that alkalies, calcium and silica show little change in the mafic and ultramafic rock types, thus many important features in these rocks are over-looked and they are merely classified as tholeiitic basalts. Secondly, it is precisely these oxides that show evidence of alteration in even low grade metamorphism. Consequently, Jenson (1976) selected Al_2O_3 , $FeO + Fe_2O_3 + TiO_2$ and MgO as the axes of the ternary plot due to their relative stability within volcanic rocks. They are much less susceptible to migration than K, Na, Ca and Si. He proposes that cation percentages rather than weight percentages be used due to the heavy atomic weight of Fe and Ti with respect to the Al and Mg atoms.

The curved line separating the tholeiitic and calc-alkaline fields corresponds closely to that of Irving and Baragar's (1971, Figure 28) AFM diagram. However, Jenson's (1976) plot divides the subalkaline rocks further into Mg-rich and Fe-rich tholeiitic basalt, and basaltic and peridotitic komatiites.

Using the discriminatory functions outlined in Appendix D, the rocks were first classified as alkaline or subalkaline (see Figure 27). All volcanic rock samples plotted either as subalkaline or were close to the dividing line between the subalkaline and alkaline fields. Sample 209 was the one exception. Thus the volcanics in the study area were classified as subalkaline. Samples 73 and 106 were not included due to high loss on ignition values of 40.1 and 10.3% respectively.

On the AFM diagram (Figure 28), two distinct trends emerged. One shows a trend of iron enrichment in the tholeiitic field and the other is within the calc-alkaline field. A comparison was then made with the Jenson Plot (1976) for subalkaline rocks (Figure 29). A distinct trend in this plot may be noted ranging from basaltic komatiites, through tholeiitic basalts, to the calc-alkaline-tholeiitic border of andesites and dacites (Figure 29).

Further classification into specific rock names according to Irving and Baragar (1971) was made in Figure 30.

A list of rock names given by each classification may be found in Table II.

Irving and Baragar (1971) suggest a further breakdown into K-rich, average or K-poor rocks. This may be seen in Figure 31. All of the samples plotted tend to be average to K-rich.

A list of all rock samples and their rock names can be found in Appendix A.

Further criteria for the classification of the basaltic komatiites included characteristics noted by Brooks and Hart (1974) and Arndt et.al.

Fig. 27 - $\text{Na}_2\text{O} + \text{K}_2\text{O}$ vs SiO_2

Legend for Variation Diagrams

- I Basaltic Komatiites
- Tholeiitic Basalt
- Calc-alkali Andesite
- x Felsic Volcanics
- x Intrusive (gabbro)
- v Varioles in the Tholeiitic Basalt

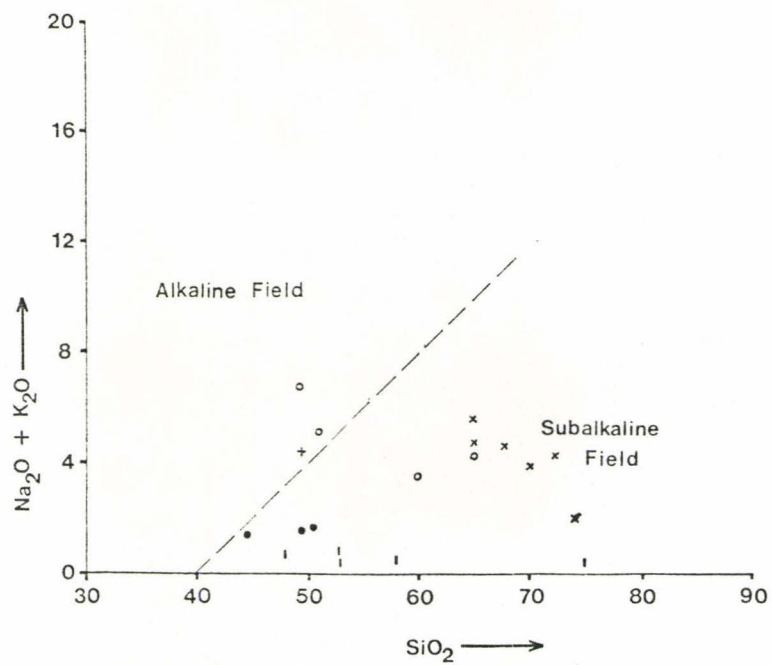


Fig. 28 - AFM diagram

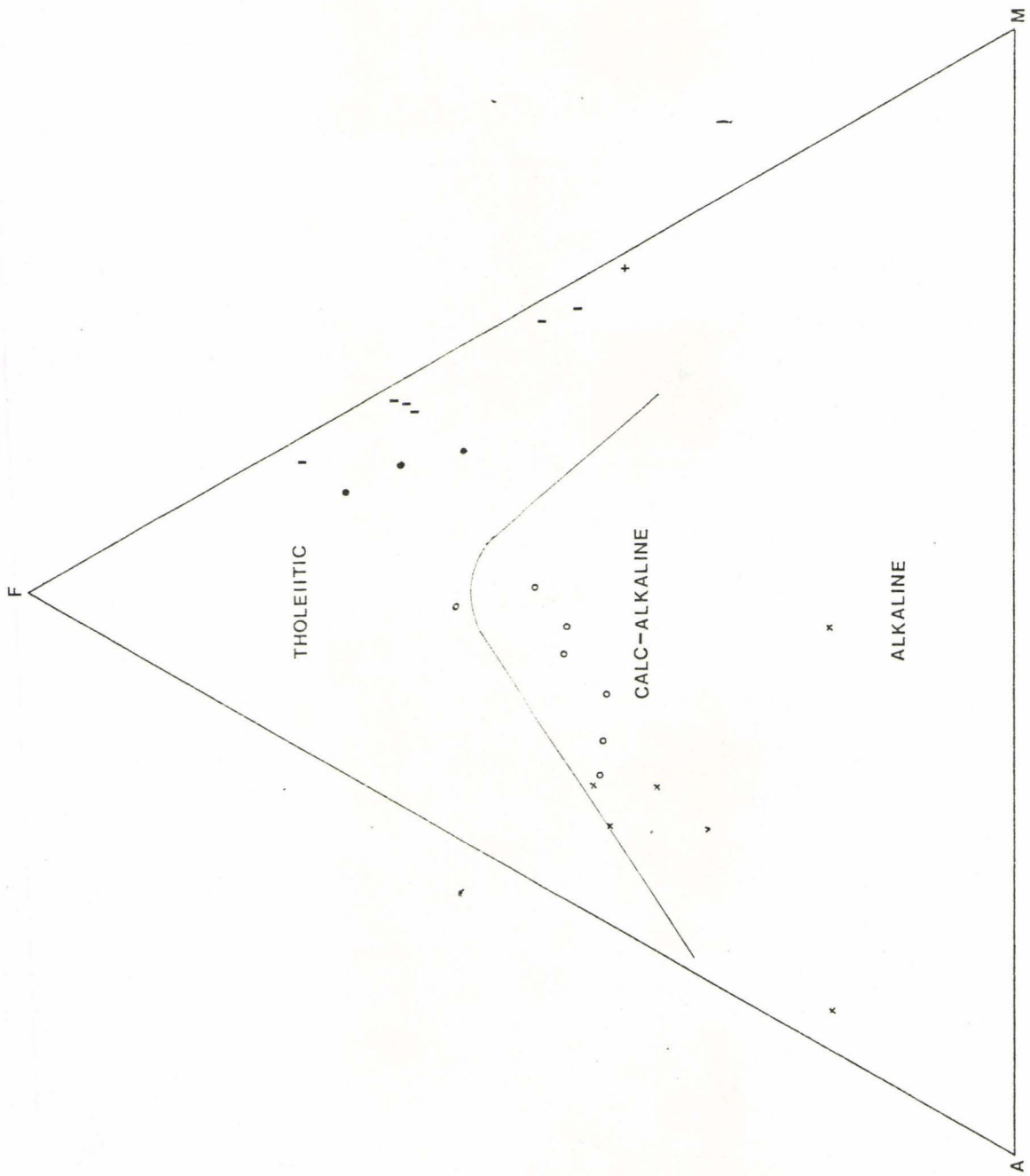


Fig. 29 - Jenson's Cation Plot

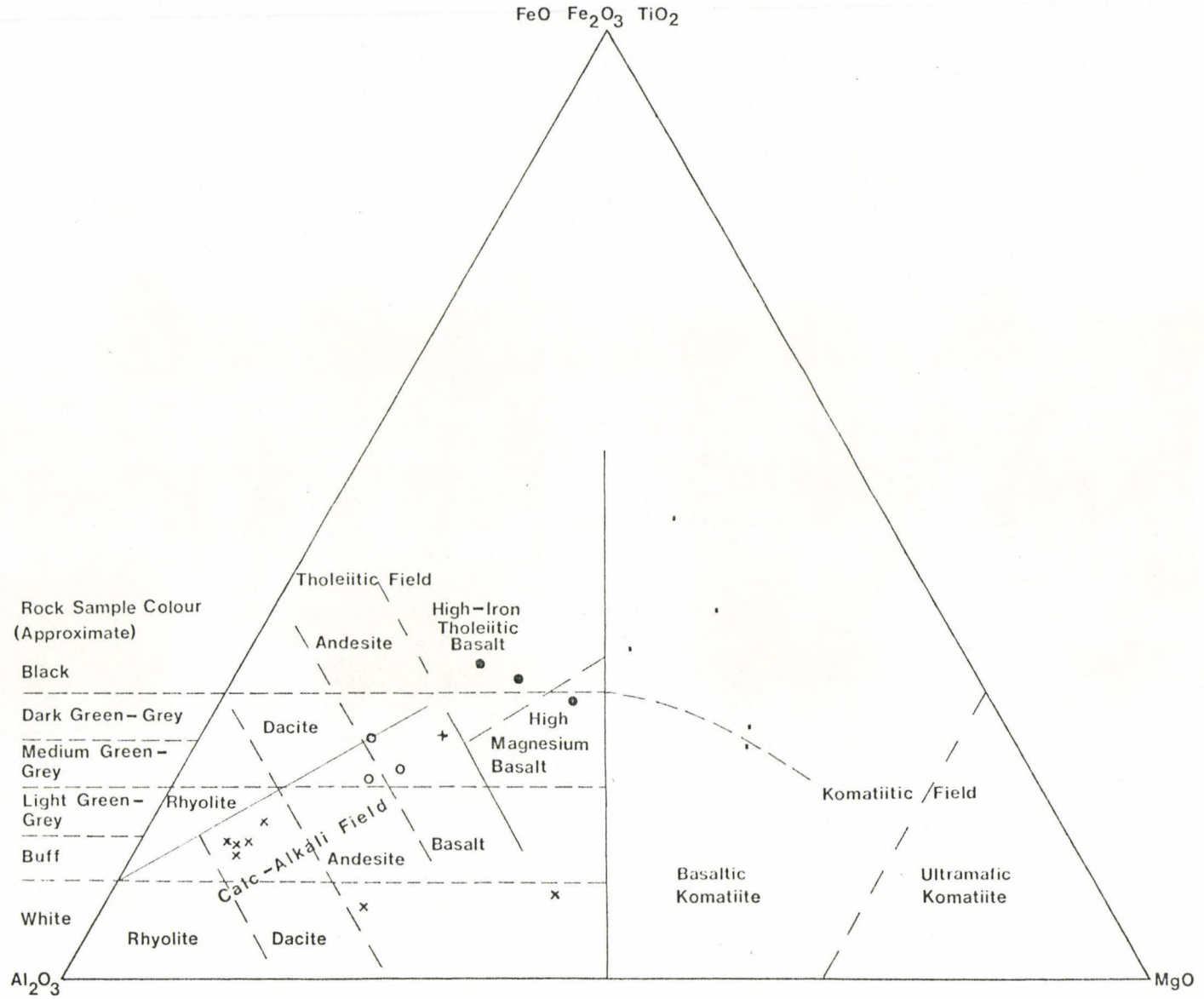


Fig. 30 - Normative C.I. vs Normative Plagioclase Composition

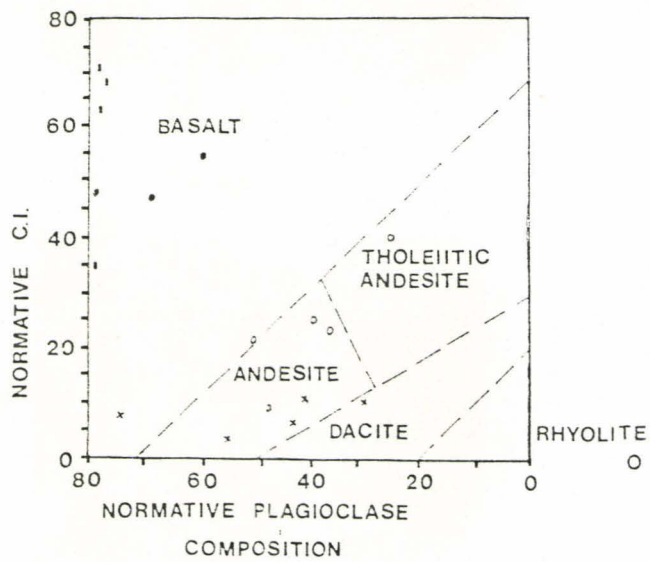
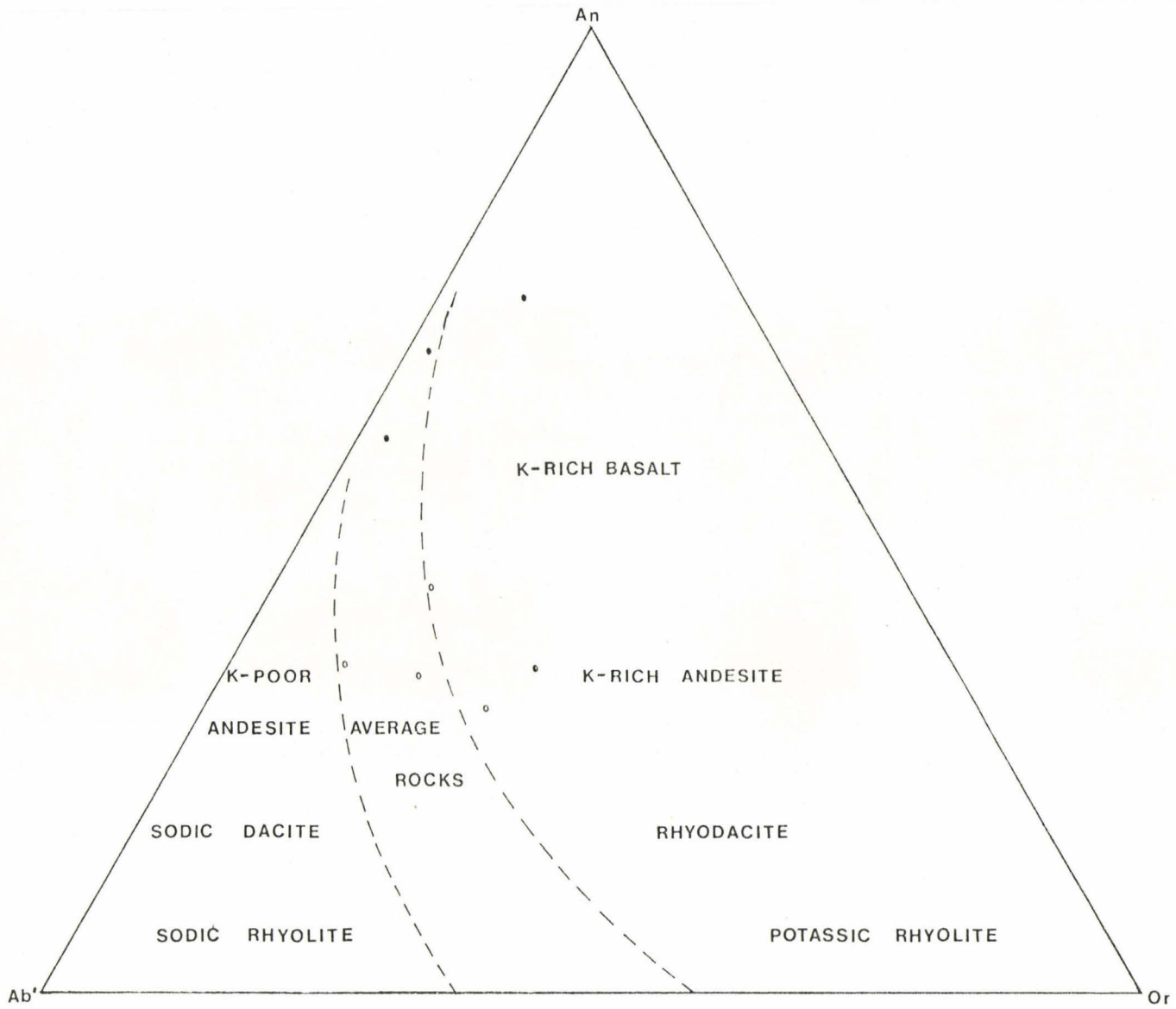


Table II Volcanic Rock Classification

Tholeiitic basalt	High Mg basalt	basaltic komatiite, petrographic evidence
Tholeiitic basalt	Basaltic komatiite	pseudo-spinifex
Tholeiitic basalt	Basaltic komatiite	micro-spinifex
Tholeiitic basalt	Basaltic komatiite	serpentinite, petrographic evidence
Tholeiitic basalt	Basaltic komatiite	pseudo-spinifex
Tholeiitic basalt	High Fe basalt	variolitic
		andesite, petrographic & field evidence
Tholeiitic basalt	High Fe basalt	variolitic
Calc-alkaline andesite	Calc-alkaline dacite	pyroclastic
Calc-alkaline andesite	Calc-alkaline dacite	pyroclastic
Tholeiitic basalt	Calc-alkaline basalt	gabbro, petrographic & field evidence
Calc-alkaline andesite	Calc-alkaline dacite	andesite, petrographic evidence
Tholeiitic basalt	Calc-alkaline dacite	pyroclastic
Calc-alkaline andesite	Calc-alkaline andesite	pyroclastic
Calc-alkaline andesite	Calc-alkaline basalt	pyroclastic
Calc-alkaline andesite	Calc-alkaline dacite	pyroclastic
Tholeiitic basalt	Tholeiitic andesite	border between basalt & andesite
Calc-alkaline andesite	Calc-alkaline basalt	andesite, petrographic evidence
Tholeiitic basalt	Basaltic komatiite	micro-spinifex
Tholeiitic basalt	Basaltic komatiite	micro-spinifex
Calc-alkaline andesite	Calc-alkaline andesite	
Calc-alkaline dacite	Calc-alkaline dacite	pyroclastic

Fig. 31 - Ternary diagram of An-Ab-Or



(1977). Brooks and Hart (194) suggested that komatiites were non-cumulative rocks with $\text{MgO} < 9\%$, $\text{K}_2\text{O} < 0.5\%$, $\text{TiO}_2 < 0.9\%$ and $\text{CaO}/\text{Al}_2\text{O}_3 > 1$. Arndt et.al. (1977) note that the average $\text{CaO}/\text{Al}_2\text{O}_3$ of Munro Komatiites is 0.84 and so a broader definition of komatiite was proposed. However, the criteria set by Brooks and Hart (1971) were met by the basaltic komatiites of the study area with one exception; the MgO content. In the broader definition proposed by Arndt et.al. (1977) the MgO content is actually not important. Textural and other chemical characteristics become the defining characteristics, and are met by the basaltic komatiites of the study area. These include spinifex texture, "blocky" pillows (polyhedral jointing), low Fe/Mg ratios, low TiO_2 at given SiO_2 and high MgO, NiO and Cr_2O_3 . A compilation of the criteria by both authors and a comparison with the data of the study area can be seen in Table III.

The use of sample 200 is questionable due to high SiO_2 values resulting from contamination of a quartz vein. Consequently, the absolute values are not reliable, but the relative values of the oxides in terms of ratios are still useful. Thin section analysis substantiates the classification.

The felsic volcanics are composed of pyroclastic rocks laid down in water as evidenced by graded bedding and slump structures. Consequently the chemical analysis is not a true indication of the chemical composition of the felsic material which was extruded, as sedimentary material would most likely have been incorporated with the volcanics. The chemistry may also have changed due to sedimentary processes. Thus the chemical analyses may have been very broad indicators of the original volcanic material, or

Table III Chemical Criteria for Komatiites as set by Brooks & Hart (1973)
Arndt et.a. (1977)

oxides (wt%)	24	76	PC31	200	206	Criteria	Author
TiO ₂	0.29	0.14	0.28	not applicable	0.16	<0.9% <1.0%	B & H A et.al.
K ₂ O	0.10	0.06	0.13	not applicable	0.34	<0.5% low	B & H A et.al.
MgO	7.41	7.49	13.40	not applicable	6.67	>9% <12%	B & H B & H
Fe/Mg	1.22	0.7	0.6	1.19	1.92	low at given Al ₂ O ₃	A et.al.
CaO/Al ₂ O ₃	1.30	3.65	1.29	1.80	2.06	>1 high	B & H A et.al.
Ni (ppm)	834	213	767	324	1036	high high	B & H A et.al.
Cr (ppm)	32.3	3120	2678	3439	3360	high high	B & H A et.al.
FeO*/(FeO+MgO)	0.67	0.55	0.51	0.66	0.66	0.65	A et.al.
Al ₂ O ₃	8.40	4.51	8.39	3.18	5.31	moderately low	A et.al.

may not be related at all.

The volcanic breccia contains blocks of quartz porphyry, indicating a high felsic content of the material which was originally fragmented. The high felsic content of the analyses is substantiated in the lapilli and ash tuff by the presence of glass and feldspar crystals. Thus the combination of the high possibility of incorporated sedimentary material in the deposits and the predominance of felsic crystals, would bias the analyses towards the felsic end. Consequently, the plotted analyses may not indicate the appropriate classification of the original volcanic material. Another point to be kept in mind is the possibility that the pyroclastic material may not be derived from a volcanic lava, but may be the surrounding country rock to the volcanic event.

Chapter IV Geochemistry

1. Introduction

A Philips, Model 1450 AHP, automatic, sequential, X-ray fluorescence spectrometer was used for whole rock and trace and trace element analyses, within the Geology Department, McMaster University for most of the samples. A 6:1 lithium tetraborate and lithium metaborate mixture (flux) to rock powder ratio was fused in Pt/Au crucibles for 3-5 minutes at 1200°C for whole rock analyses. The major elements Si, Al, total Fe, Mg, Ca, Na, K and the minor elements Ti, Mn and P were analysed using a Cr X-ray tube. The trace elements Rb, Sr, Y, Zr, Nb, Ni, Zn, Pb, As, Cu, Cr, Co, and S were analysed in the form of a pressed powder disc using a Mo tube.

All samples were analysed by the author with the exceptions of sample PC31 (Pat Cowan, McMaster University) and samples JP485 and JP488 (Ontario Geological Survey for J. Pirie). See Appendix C for analytical methods and Appendix D for the individual analyses.

2. Major Elements

Chemical Variation

The range and variation of the major and minor oxides of the volcanic rock types within the study area are given in Table IV. The felsic volcanics contain the most silica, as would be expected by definition. In order of decreasing silica content, the volcanics are: felsic volcanics, andesites, komatiites and basalts. Overlaps in the silica content do exist between all volcanic classifications. All are over-saturated with respect to normative quartz, sample 209 being the exception. For individual cation norms, see

Table IV Chemical Variations of Volcanic Rocks (wt%)

Classification of analyses	Komatiitic Basalt 4	Tholeiitic Basalts 3	Andesites 4	Felsic Volcanics 6
SiO ₂	47.95 - 57.84	44.69 - 50.78	49.44 - 64.95	64.68 - 73.98
TiO ₂	0.14 - 0.29	0.31 - 0.79	0.42 - 0.76	0.19 - 0.46
Al ₂ O ₃	4.51 - 8.40	9.82 - 13.68	15.83 - 17.31	9.46 - 15.41
Fe ₂ O ₃	1.64 - 1.79	1.81 - 2.29	1.92 - 2.26	1.69 - 2.01
FeO	5.64 - 16.79	8.51 - 11.86	2.59 - 7.00	0.00 - 3.00
MnO	0.20 - 0.45	0.28 - 0.36	0.14 - 0.18	0.02 - 0.21
MgO	6.67 - 13.40	5.22 - 6.42	1.69 - 4.30	0.31 - 3.64
CaO	10.81 - 16.46	10.35 - 13.57	3.38 - 7.04	0.95 - 3.62
Na ₂ O	0.33 - 0.60	0.96 - 1.52	2.09 - 4.03	1.26 - 3.91
K ₂ O	0.06 - 0.34	0.06 - 0.17	1.17 - 3.00	0.76 - 3.11
P ₂ O ₅	0.02 - 0.04	0.02	0.02 - 0.30	0.02 - 0.06

Appendix F. The komatiites tend to be high in silica when compared with the Barberton, South Africa and Munro and Dundonald Townships, Ontario komatiites ($\text{SiO}_2 = 39-46\%$ compared to $48-58\%$ in the study area). However, these komatiites are ultramafic ($\text{MgO} = 23-34\%$). (Pyke et.a., Table 1, 1973). Thus a higher silica content in the basaltic komatiites of the study area may be expected. Local silicification of the rocks around the gold mines of the Red Lake area has also been noted by Pirie (personal communication, 1979). A gold mine (McKenzie Island gold mine) does exist on McKenzie Island near the study area, thus silicification during metamorphism may also be a possibility.

Titanium exhibits a continuous decrease from the tholeiitic basalts and andesites (about on par) to the felsic volcanics, followed by the komatiitic basalts. The one exception is sample 21a which is a high Mg-tholeiitic basalt by Jenson's (1976) classification and tends to represent a transition between the two series. All of the rocks are low in titanium, which is characteristic of island arc volcanics (Hyndman, 1972). This trend was observed in the data presented by Pearce and Cann (1973).

A discriminatory feature between tholeiitic and komatiitic basalts pointed out by Arndt et.al. (1977) and Brooks and Hart (1974) emerges for the study area. This is illustrated in Figures 52 and 53. For any composition of the two series, which may be specified by MgO or SiO_2 content, the TiO_2 content of the tholeiitic basalt exceeds that of the komatiitic basalt. The TiO_2 content of the andesites and basalts are the same. The andesites are consistently higher in SiO_2 and lower in MgO than the basalt, which follows by definition.

Fig. 32 - TiO_2 vs MgO

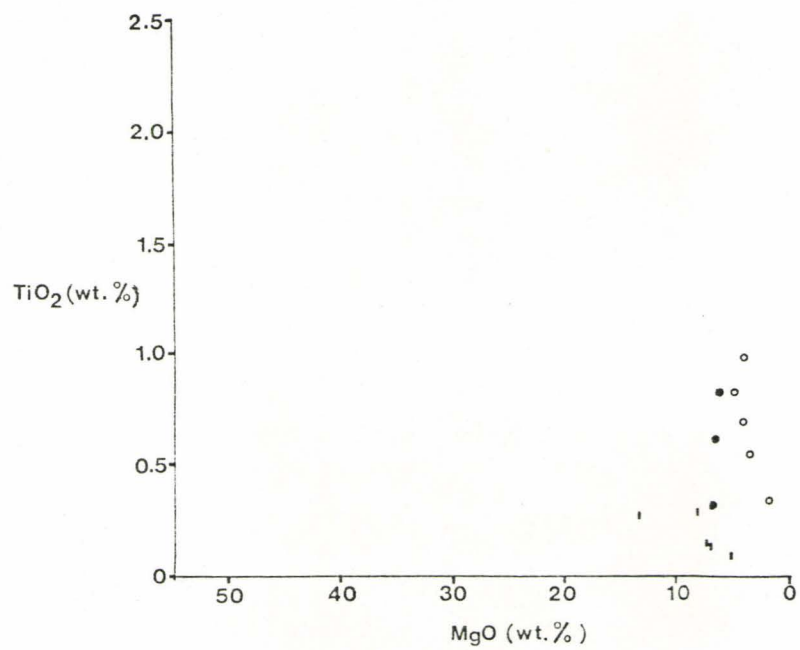
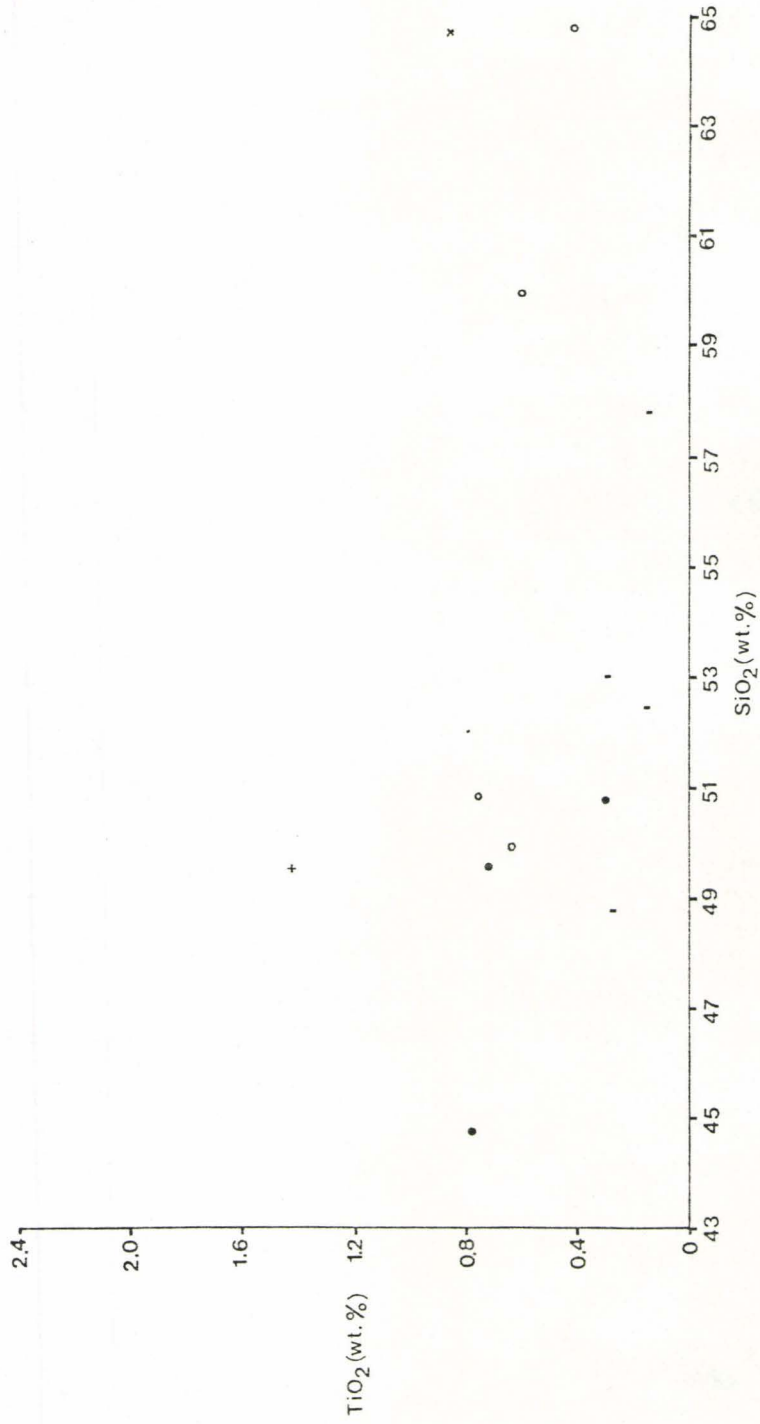


Fig. 33 - TiO_2 vs SiO_2



Another discriminatory feature is that of TiO_2 vs Al_2O_3 as illustrated in Figure 34. The basaltic komatiites are consistently lower in TiO_2 and Al_2O_3 than the tholeiitic basalts and the andesites. Thus the komatiitic basalts are clearly distinguished from the "normal" basalts.

A diagram found useful for distinguishing between the komatiitic and tholeiitic series by Naldrett and Mason (1968) and Arndt et.al. (1977) is the Al_2O_3 vs $\text{FeO}/(\text{FeO} + \text{MgO})$ plot, where FeO equals total iron (Figure 35). Komatiites consistently have lower $\text{FeO}/(\text{FeO} + \text{MgO})$ ratios than tholeiites of similar Al_2O_3 content. Arndt et.al. (1977) state that this relationship holds true for both noncumulate and cumulate rocks as well as for mafic rocks in which there is a large degree of compositional overlap between tholeiites and komatiites. The basaltic komatiites within the study area fall near the pyroxenitic field of the Munro Komatiites, but have slightly higher $\text{FeO}/(\text{FeO} + \text{MgO})$ ratios. The tholeiitic basalts fall in the tholeiitic field.

MgO decreases steadily from the basaltic komatiites, through the tholeiitic basalts into the andesites, and a slight though not as distinct decrease from the andesites to the felsic volcanics. MgO is very strongly enriched in the silicate minerals which separate from the magma during the early stages of crystallization in the ultrabasic rocks. Thus the first products of magmatic differentiation tend to be high in Mg^{2+} (Rankama and Sahama, 1950). Mason (1958) notes that ferromagnesian minerals are individual continuous series in which the early-formed crystals are magnesium-rich and the late-formed iron-rich. Thus, most of the magnesium is bound up in the pyroxene of the komatiites and the olivine and pyroxene of the basalts.

Fig. 34 TiO_2 vs Al_2O_3

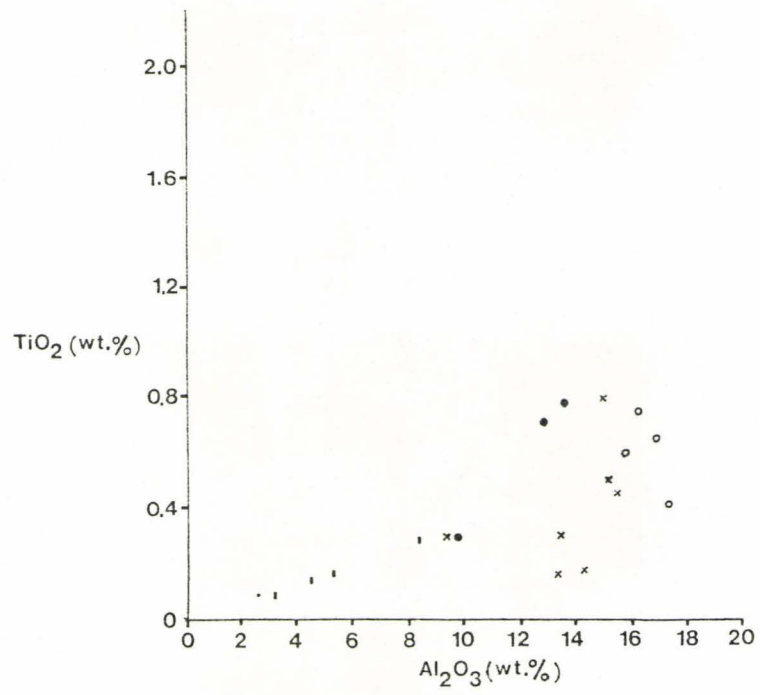
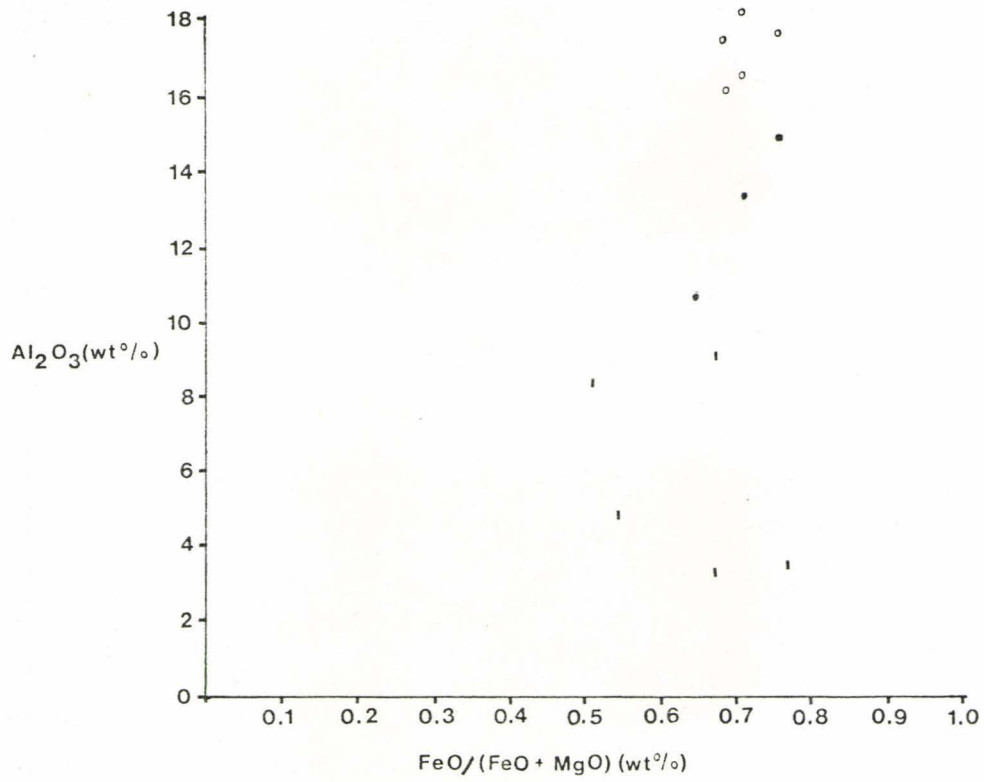


Fig. 35 Al_2O_3 vs $\text{FeO}/(\text{FeO} + \text{MgO})$



This explains the decrease in MgO with possible differentiation from the komatiites, to the tholeiites, to the calc-alkalies.

CaO shows a similar trend to that of MgO. The calcium content of minerals which crystallize early is high, and decreases with differentiation. Thus early crystallizing pyroxenes and feldspars have a high calcium content (Carmichael et.al., 1974). This therefore accounts for the systematic decrease of calcium in the rocks of the study area. Calcium is also a rather mobile ion and is affected by metamorphism (Rankama and Sahama, 1950). Consequently, metamorphism may be isochemical.

The high calcium content of the basalts can most likely be accounted for by the presence of actinolite-tremolite in the rock. This would also account for the high iron and magnesium content. The original and most abundant pyroxene may therefore have been augite.

The iron enrichment of the basalts may be due to processes similar to that of the Skaergaard intrusion. Shelley (1975) mentions that the iron enrichment of Skaergaard is due to the initial crystallization of a diopsidic augite and Mg-rich orthopyroxene. With fractionation both the augite and pigeonite become more Fe-rich until eventually pigeonite ceases to crystallize. Similar compositional trends of Fe-enrichment are common and known for a large number of rock suites (Shelley, 1975).

The normative alkali feldspar reflects the amount of alkalies present in the rocks. They are the lowest in the komatiitic basalts illustrated by the lowest normative alkali feldspar. Due to extensive alteration of the rocks to sericite and chlorite, a modal comparison was not possible.

3. Trace Elements

Chemical Variation

Variations in the abundances of the trace elements are of importance in evaluating the evolution of the igneous rocks as they tend to be good indicators of differentiation in magmatic processes (Schnetzler and Philpotts, 1968). In an attempt to deduce the original tectonic environment of basic volcanic rocks, comparisons of trace element concentrations of the unknown rock with concentrations of present day volcanic rocks of known tectonic settings, will also be made (Pearce and Cann, 1973).

The ranges and variations of the trace elements in the various volcanic rocks are given in Table V. The individual analyses are given in Appendix E.

Rb shows a wide range of chemical variation, a break existing between the basalts on the one hand and the andesites and felsic volcanics on the other. This is reasonable due to the affinity of Rb for potassium minerals (Mason, 1958). It is also incompatible with respect to the various anhydrous phases proposed for mantle rocks, namely olivine and pyroxene (Carmichael et.al., 1974). Thus Rb is virtually non-existent in the mafic volcanics and of higher concentration in the felsic volcanics.

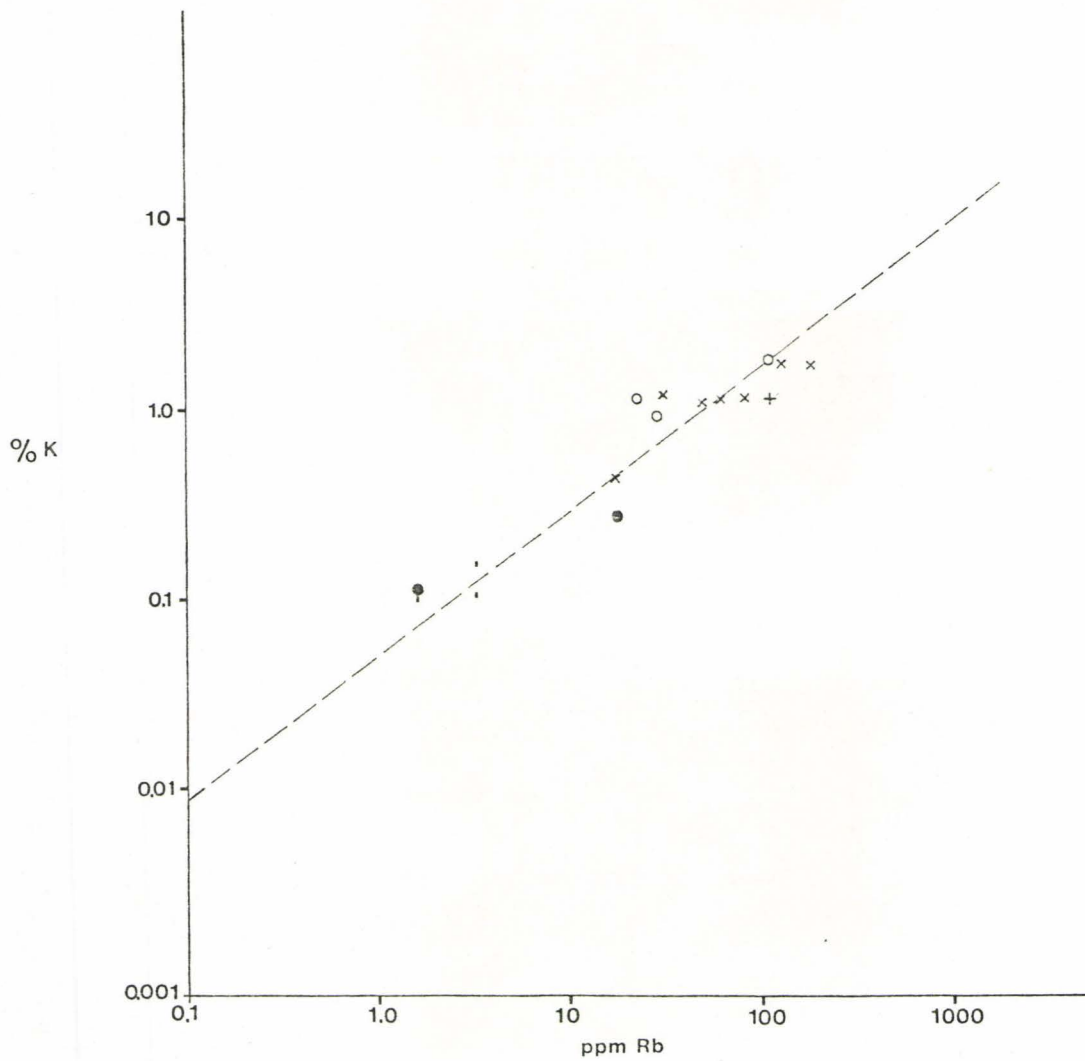
A plot of %K vs Rb (ppm) gives a linear trend as seen in Figure 36 (the slope of the line being close to 45°, slope = 0.714). Average R for the basalts is 310 and 190 for the andesites and felsic volcanics, where $R = 10^4 \%K / \text{ppmRb}$.

Shaw (1970) notes that there is no consensus of opinion as to whether

Table V Trace Element Variation of Volcanic Rocks (ppm)

Classification of analyses	Komatiitic Basalt 6	Tholeiitic Basalt 3	Andesite 5	Felsic Volcanics 6
Rb	0 - 7	2 - 25	46 - 122	31 - 125
Sr	0 - 62	100 - 188	144 - 759	82 - 304
Y	0 - 6	8 - 15	1 - 31	6 - 25
Zr	16 - 30	38 - 74	50 - 145	100 - 160
Nb	1 - 12	3 - 13	4 - 16	12 - 18(5 analyses)
Ni	213 - 1036	200 - 262	15 - 225	10 - 42
Zn	51 - 87	83 - 132	44 - 87	34 - 77
Pb	7 - 13	10 - 11	12 - 29	9 - 28
As	0 - 15	0	0 - 33	0 - 19
Cu	3 - 10	27 - 295	6 - 51	7 - 14
Cr	2678 - 3439	574 - 3498	39 - 255	6 - 330
Co	36 - 124	50 - 64	29 - 39	7 - 28
S	121 - 330	320 - 476	242 - 632	100 - 859
γ/Rb	0 - 403	70 - 248	176 - 360	111 - 402
γ/Sr	0 - 0.113	0.02 - 0.13	0.09 - 0.37	
γ/Nb	0 - 5	1 - 5	1 - 3	0 - 1(5 analyses)

Fig. 36 K vs Rb



the ratio $R = K:Rb$ remains constant during igneous and quasi-igneous crystallization. Erlank (1968) states that the R does not vary significantly in igneous rocks, and remains relatively constant during the main stages of igneous differentiation, showing a decrease only in the final stages or in highly fractionated granitic rocks. After some discussion Shaw (1970) concludes that $K-Rb$ relations in igneous rocks can take one of three forms; the main trend ($R = 200-400$), the oceanic tholeiitic trend ($R = 1000-3000$) or the pegmatitic-hydrothermal trend ($R = 20-50$). The value of R decreases slightly as the concentrations of K decrease or Rb increases during the main trend, and the value of R appropriate to a particular K concentration varies from suite to suite.

Amphiboles have a median R value of 110, plagioclase in common igneous rocks of 300-400 and muscovite, K -feldspar, olivine and pyroxene 200-300 (Shaw, 1970). Thus, the higher R value in the basalts may be related to the high amphibole content. In any case, the R value for the suite of rocks as a whole, does not vary greatly from the overall rock values of the main trend, and a decrease in this case may be due to fractionation. Shaw (1970) also mentions that ultramafic rock types appear to lie on the main trend. The main trend defined by covariance analysis is given by basic rocks whose main phases are olivine, pyroxene, plagioclase and by more silicic rocks with two feldspars, quartz, biotite and hornblende. Thus the rocks of the study area should indeed follow the main trend as indicated.

Sr is markedly depleted in the basaltic komatiites with respect to the other rock types. Strontium accompanies calcium constantly in minerals and rocks of igneous origin and may replace potassium in many minerals. It will often substitute for calcium in the plagioclases and

potash feldspars, as well as in the calcium-bearing pyroxenes and amphiboles (Rankama and Sahama, 1950). The concentration of strontium increases as crystallization proceeds, which Mason (1958) interprets as an admittance of strontium in place of calcium. However, Mason (1958) also notes that strontium is present only in insignificant amounts in augite suggesting that the pyroxene structure does not readily accommodate the ion. Thus, the low Sr concentration of the basalts may be due to the presence of pyroxene even though the calcium content is higher than that of the felsic volcanics.

Arth et.al. (1977) note that the increase of Sr is a function of MgO, and is consistent with a fractional crystallization model for tholeiites and komatiites. As MgO decreases, Sr becomes enriched, which is consistent with its solid/liquid partition coefficients for olivine and clinopyroxene. This also seems to be the case in the study area, and may be tied into the high presence of amphibole which is in fact, altered serpentine.

Y, Zr, and Nb are all lowest in the basaltic komatiites and highest in the andesites and felsic volcanics. These elements are known to concentrate in later stage "residual" magmas in rock series which are considered to be developed by fractional crystallization (Rankama and Sahama, 1950).

Ni and Cr are known to be highly concentrated in komatiites. This trend is certainly evident from the values on Table V. The high Cr value of the tholeiitic basalt is from sample 21a, the high Mg-basalt, intermediate between the two series. Naldrett and Turner (1977) have demonstrated that basaltic komatiites at Yakabindie, Western Australia are characterized by high contents of Ni and Cr in comparison with tholeiites from the same area

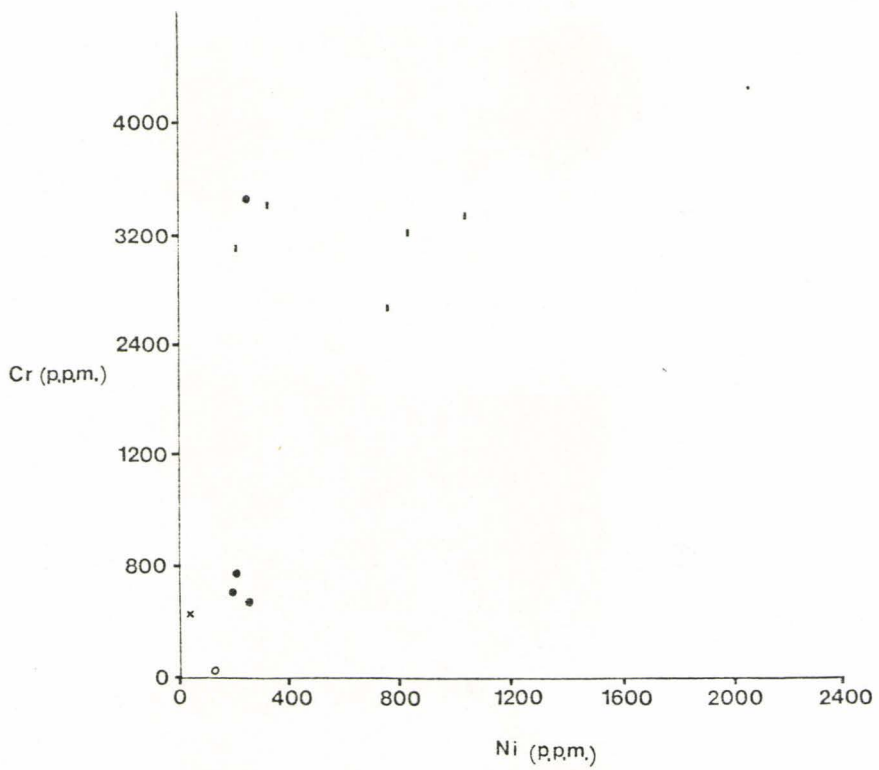
(Naldrett and Cabu, 1977) is strongly enriched in ultramafic rocks, concentrating in olivine and hypersthene and to a lesser extent in augite. Cr separates from the magma during the earliest stages of differentiation, and is strongly enriched in the early crystallates. It is especially high in fosterite-rich olivines and clinopyroxene (Rankama and Sahama, 1950), and chromite. However, chromite was not observed in the thin sections. Thus, the chrome must be in the amphibole (altered pyroxene).

The relationship of Cr and Ni with respect to the komatiites and the tholeiitic basalts and andesites is illustrated in Figure 37. The Cr content appears to be a good distinguishing parameter between the two series for the study area, being much higher in the basaltic komatiites than the tholeiitic basalts. Again 21a is the exception due to its intermediary position.

Co tends to be slightly higher in the basalts than the andesites and volcanics. It is known to vary linearly with magnesium over a wide range of concentrations (Rankama and Sahama, 1950) (Mason, 1958), and so may be accounted for by the decreasing trend of MgO in the same direction.

Zinc, arsenic, copper and sulphur show little variation. Due to the affinity copper has for sulphur, their relationship is not surprising. Pirie (personal communication, 1979) also noted a low As level in the rocks of the Red Lake area.

Fig. 37 Cr vs N



Chapter V Petrogenesis

The Southern Superior Province of the Canadian Shield is the earth's largest continuous terrane with major low-rank metamorphic (greenschist) components. What Goodwin (1977) terms cratons and basins, are found mutually arranged in high-to low-grade metamorphic terranes of gneiss and greenstone belts (and associated rocks) respectively.

The granite-greenstone belts are composed of three main sequences. The first sequence is the lowermost ultra mafics (dunites, peridotites and komatiites) interlayered with tholeiites, minor pyroclastics, and chemical sediments. The second sequence is a greenstone unit consisting of cyclic sequences of tholeiite, andesite, dacite and rhyolite. Associated, are increasing abundances of clastic metasediments, pyroclastics and iron-formations towards the top of the cycle. The third sequence consists of an upper metasedimentary group of turbidites, fluvial and metasedimentary rocks, iron-formation, and chert. Shallow marine carbonates may be associated (Longstaff, 1977; a summary of available literature).

Multiple deformation and thermal events mark the granitic and gneissic rocks of most of the gneiss belts, accompanied by interlayered, igneous complexes and supracrustal sequences containing amphibolite, felsic metavolcanic and metasedimentary rocks. (Longstaff, 1977).

The crustal evolution of these Archean rocks has long been under considerable debate. Much geochemical evidence favours island arc models and so plate tectonism. This is in keeping with the evidence from the study area (Longstaff, 1977).

Tectonic Environment

π , Zr, Y, Nb and Sr may be useful as indicators of tectonic style schemes as they have a much greater variation in concentration between samples of different magma types than between samples of the same magma type. Of these elements, Ti, Zr, Y and Nb have been suggested as insensitive to processes of alteration. Sr can be noticeably affected by some types of greenschist facies metamorphism (Pearce and Cann, 1973). Pearce and Cann (1973) proposed a basalt classification based on the following variation diagrams:

1. Ti-Zr; valid for fresh and metamorphosed basalts;
2. Ti/100-Zr-Yx 3; valid for fresh and metamorphosed basalts;
3. Ti/100-Zr-Sr/2; valid for unaltered basalts

(Longstaff, 1977) (Pearce and Cann, 1973).

They suggest that analysis first be plotted on the second variation diagram as it appears to be the most accurate for determining if the basalts are "within-plate" basalts (ocean island and continental basalts). The other magma types (if they aren't "within-plate" basalts) are best separated using the third variation diagram. However, the first diagram should be used for altered samples. The variation diagrams listed above, 2, 3, and 1, are illustrated in Figures 38, 39 and 40 respectively. The data points which do not lie in any of the fields are komatiitic and the high MgO tholeiite (Figure 40). The andesites were also plotted in an attempt to determine their relationship with the tholeiitic basalts. They fall into the designated fields with the tholeiitic basalts, the one exception being sample 140 in Figure 38. The tholeiitic basalts and andesite data points all plot within the island arc tectonic environment in each variation diagram. Due to alteration, Figure 40 should be the most reliable indication of tectonic environment. The tholeiitic basalts plot in or on the border to the "A"

Fig. 38 Ti/100 - Zr - YX3

A = low K tholeiites (island arc environment)

B = ocean floor basalts (ridge environment) and the field of
overlap for A and C

C = calc-alkali basalts (island arc environment)

D = ocean island and continental basalts (within-plate environment)

(from Pearce and Carn, 1973)

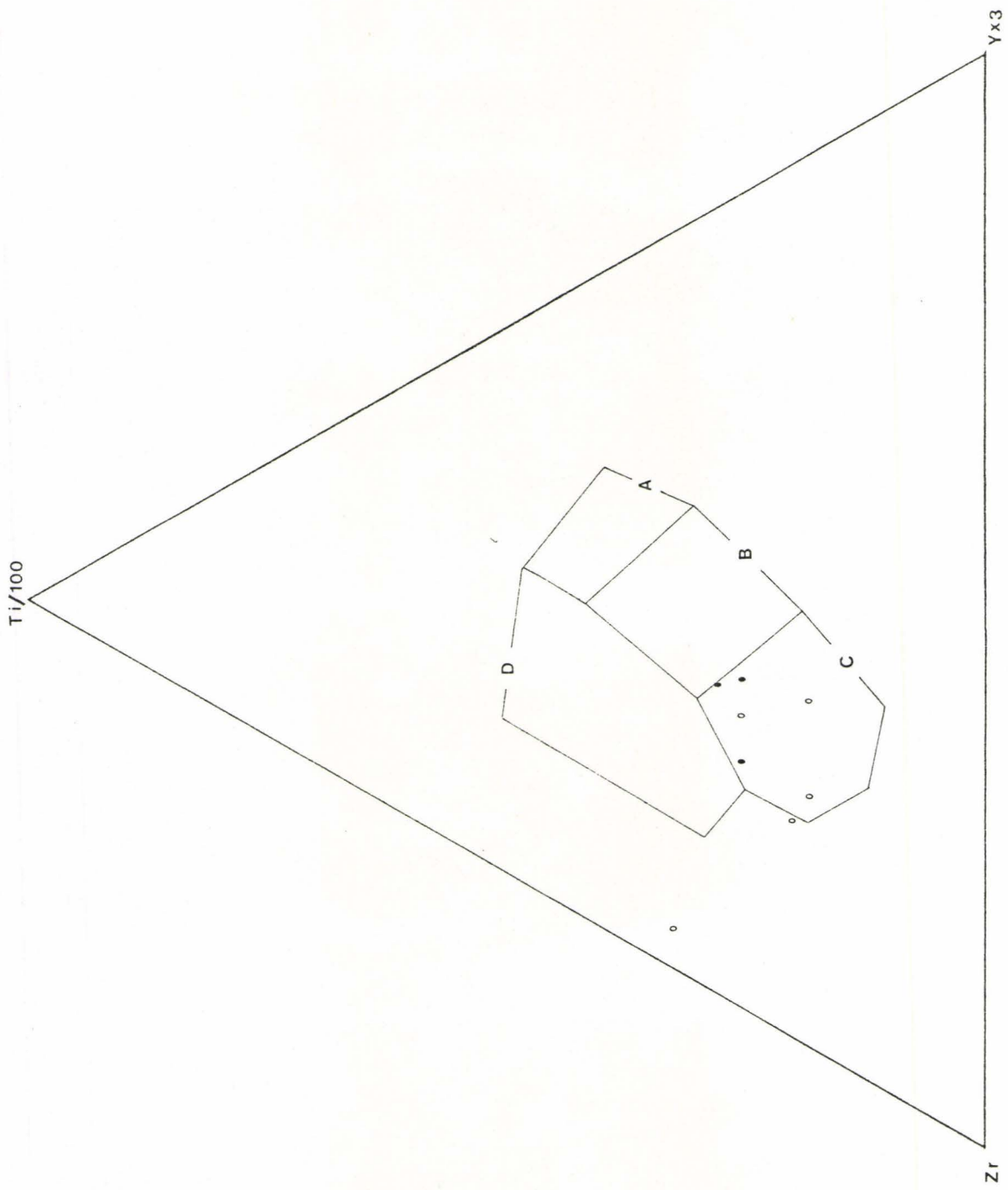


Fig. 39 Ti/100 - Zr - Sr/2

A = low K tholeiites (island arc environment)

B = calc-alkali basalts (island arc environment)

C = ocean floor basalts (ridge environment)

(from Pearce and Cann, 1973).

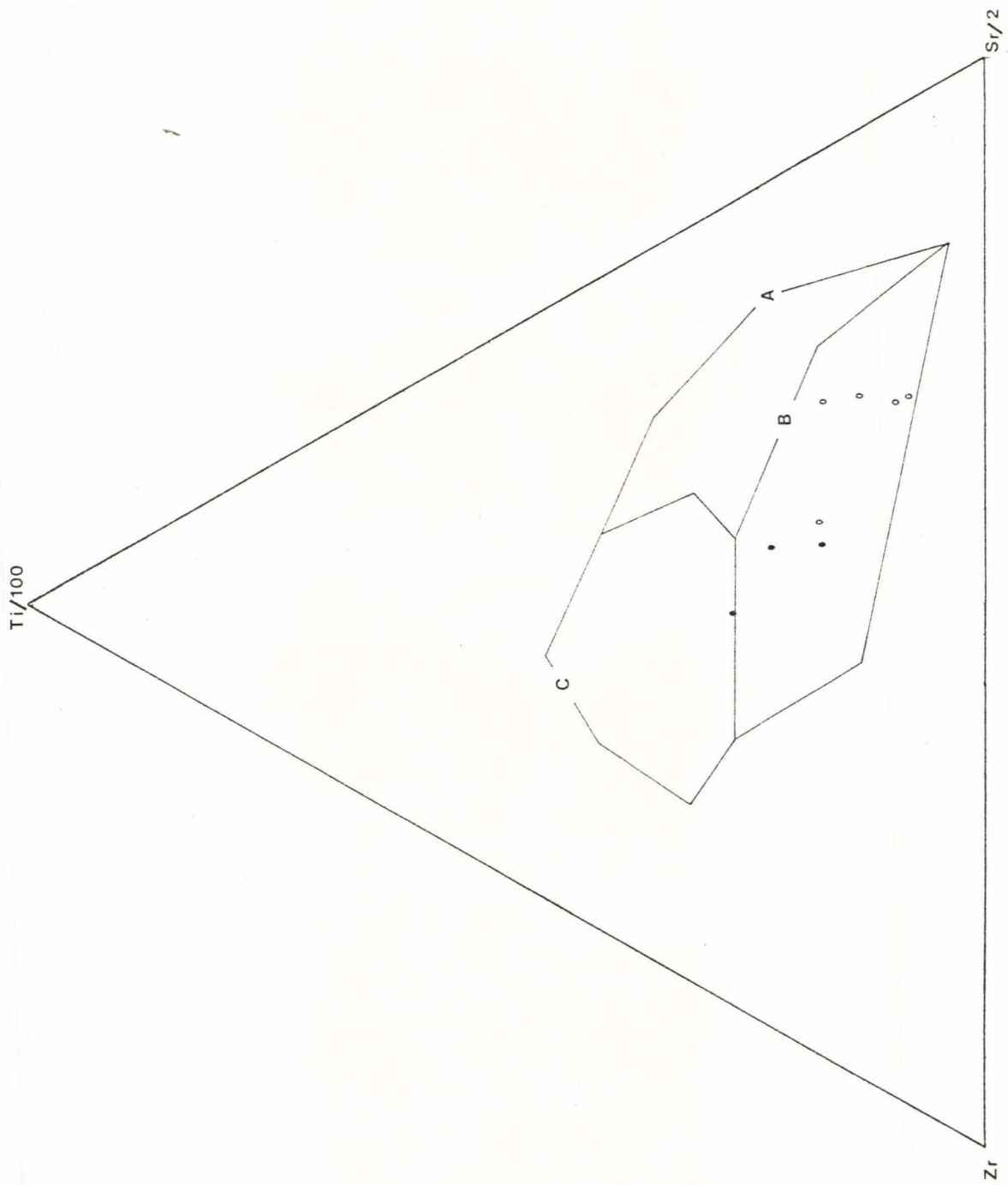


Fig. 40 $Ti \times 10^3$ vs Zr

A = low K tholeiites (island arc environment)

B = field of overlap for A, C and D

C = calc-alkali basalt (island arc environment)

D = ocean floor basalts (ridge environment)

(from Pearce and Cann, 1973)



fields, which is designated for low K tholeiites, and the andesites in the "C" field designated for calc-alkali basalts. This would therefore appear to substantiate the calc-alkali nature of these rocks.

Longstaff (1977) points out that the possibility of lower Y levels in the Archean basalts than in modern basalts may exist. The classification scheme by Pearce and Cann (1973) is based on the premise that the trace element geochemistry of the two is similar. Thus, if the Archean mantle contained a different level of Y, (and Zr, Ti or Sr for that matter) than it does now, source conditions rather than tectonic environment may be reflected.

The Tholeiitic Basalt Calc-alkali Andesite Problem

Pirie (personal communication, 1979) suggested the possibility that the calc-alkali andesites are in fact altered tholeiitic basalts. A look at Figure 28 brings out the relationship between the two rock types. The andesites tend to plot within the calc-alkali basalt field on the Jenson Plot, reasonably close to the tholeiitic-calc-alkali field border. Thus, any slight alteration of the "andesites" in terms of iron and titanium depletion would shift these rocks into the calc-alkali field. However, a definite separation of the two fields does exist in Figure 27, the AFM diagram. The similarity between the "andesites" and the tholeiitic basalts, along with the differences are exemplified in Figures 32-40.

The similarities are:

1. similar TiO_2 values (Figures 32,33,34);
2. similar $\text{FeO}/(\text{FeO} + \text{MgO})$ values (Figure 35);
3. similar K/Rb ratios (plot in the same group) (Figure 36);
4. similar Cr and Ni values (Figure 37);

5. plot in the same field in Figures 38 and 39. The differences between the two rock types are:

1. different SiO_2 content (Figure 32);
2. different MgO content (Figure 33);
3. different Al_2O_3 content (Figures 34,35);
4. plot in different fields in Figure 40.

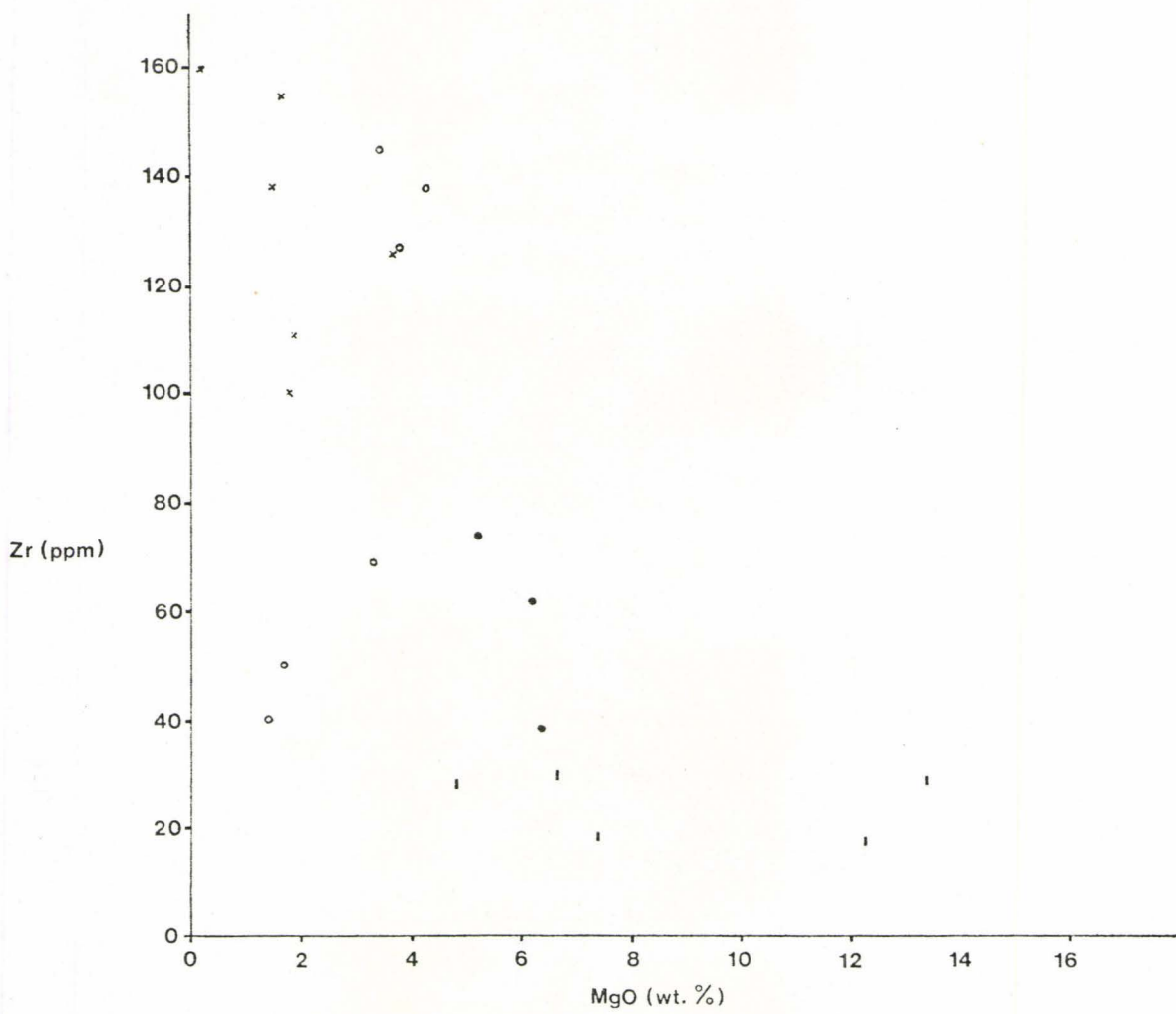
Zirconium is thought to be an indicator of magmatic differentiation, the higher values indicating greater differentiation as it tends to be left with the residual magma. The relationship of Zr vs MgO is illustrated in Figure 41. The "andesites" on this diagram are divided into two factions; those on par with the basalts and those indicating further differentiation. Thus it would appear that the "andesites" were formed in either two pulses, from different sources, or some are altered basalts and some are true andesites.

In the field, the "andesites" and tholeiitic basalts are virtually indistinguishable. Both are pillowed or massive, but the andesites tend to be greyer in colour. Both may contain varioles.

The andesites are porphyritic in this section, which is characteristic for andesites. The plagioclase composition is An_{40} - An_{48} which is on the high end for andesites and low for porphyritic andesite (Williams et.al., 1954). It is between the average composition of andesites and basalts, and so is not characteristic for either.

From the limited evidence given thus far, the possibility of the "andesites" being altered tholeiitic basalts certainly exists. More information beyond the scope of this thesis is required.

Fig. 41 - Zr vs MgO



Genesis of the Basaltic Komatiites and Tholeiitic Basalts

Arth et.al. (1977) speculate that the tholeiitic and komatiitic lavas are genetically related due to the close association of the two rock types in many localities. Munro Township contains tholeiitic volcanic rocks of basaltic to andesitic composition interlayered with komatiitic rocks (Arndt et.al., 1977) Arth et.al., (1977) state that an association is possible if the mantle peridotite that melted to yield tholeiitic lava was then remelted to yield komatiitic liquids. One tectonic model would involve a rising mantle diapir. The rise of a diapir of garnet peridotite along an adiabatic gradient would result in increased percentages of melt. The melts would then be successively tapped as they formed, the tholeiites being removed first, followed by pyroxenitic komatiites and peridotitic komatiites.

Geochemical trends cited in the previous chapter would tend to suggest a relationship between the basaltic komatiites and the tholeiitic basalts. The trends between the two rock types are summarized below.

1. decreasing Fe^{2+} (from komatiite to tholeiitic basalt)
2. decreasing MgO
3. decreasing CaO (Questionable due to later alteration)
4. increasing Sr
5. increasing Y, Zr, Nb
6. decreasing Ni and Cr
7. decreasing Co
8. general iron enrichment trend illustrated in the Jensen Cation Plot
9. Al_2O_3 enrichment

10. TiO_2 enrichment
11. high Mg-basalt, sample 21a intermediate between the two rock types on most variation diagrams
12. K/Rb ratios on the same slope (Figure 36)

The trends suggest that the komatiitic lava was extruded prior to the tholeiitic lava which is contrary to the hypothesis put forward by Arth et.al. (1977). It would appear that the mafic volcanic rocks in the study area may therefore have originated from more than one source. The trends do suggest a differentiation "direction" to the south. This is in direct contrast to the younging direction indicated by the felsic volcanics to the north. Thus in conclusion, it would seem that the komatiitic and tholeiitic lavas originated from different sources.

The Felsic-Mafic Volcanic Relationship

An aeromagnetic survey was carried out by the O.G.S and indicated one rock unit or sequence immediately to the north of the study area overlying both the felsic and mafic volcanics. Consequently it would appear that the felsic volcanics originated from a different source direction than the mafics as they are situated normal to the strikes of the mafics indicated by the pillow basalts. The two rock units therefore, most likely represent a facies change which was then overlain by one, relatively continuous, homogeneous rock unit.

Chapter VI Summary and Conclusions

The volcanic rocks of the study area are characterized by a diversity in composition ranging from felsic volcanics to basaltic komatiites. Minor intrusions of quartz porphyry, gabbro and serpentinite are evident. Chemical metasediments are interlayered with the meta-volcanics and may be accompanied by clastic metavolcanics. These sediments provide the only reliable horizon markers in the area.

Evidence from chemical and field variations indicate that the rock can be divided into three main volcanic rock types and possibly four. They are: basaltic komatiites, tholeiitic basalts, felsic, volcanics and possibly calc-alkali andesites. The possibility that the "calc-alkali andesites" represent altered tholeiitic basalts does exist.

Strike directions vary from north-east to east to southeast indicating the possible presence of a large scale structure of some sort, such as a plunging anticline or syncline.

A younging direction to the north west is indicated by graded bedding within the felsic volcanics and a general "fining" sequence from volcanic breccia on the north shore of McKenzie Island to ash tuffs on the most northeasterly island of the study area. The volcanic bombs are basically of one composition; quartz porphyry - and the lapilli tuff and ash tuff is dominated by plagioclase and quartz "eyes". Occasional pumice and mafic rock fragments are scattered throughout the area.

The mafic volcanics exhibit flow-top breccias along the northern "border" of the study area, and volcanic pillows oriented parallel to this

strike direction. Tops on the pillows could not be determined with any degree of confidence due to deformation. As indicated previously, geochemical evidence indicates a possible general differentiation "direction" towards the south, which may therefore indicate more than one source for the two volcanic rock types. Any conclusions concerning these two "trends" cannot be made without further field information and study.

APPENDIX

Appendix A Rock Samples and their Names

21a	High Mg basalt
21b	Basaltic komatiite
24	Basaltic komatiite
PC31	Basaltic komatiite
73	Serpentinite
76	Basaltic komatiite
80	High Fe basalt
99	Lean iron formation
105	Quartz porphyry
106	Andesite
108	High Fe basalt
112	Pyroclastic
135	Pyroclastic
136	Pyroclastic
137	Pyroclastic
140	Andesite
150	Pyroclastic
155	Pyroclastic
160	Pyroclastic
161	Pyroclastic
163	Gabbro
166	Basaltic Andesite
188	Andesite
195	Slate

Appendix A continued....

200	Basaltic komatiite
205	Wacke
206	Basaltic komatiite
209	Andesite
JP485	Pyroclastic
JP488	Variolites in the basalt
JP290	Basalt
JP294	Basaltic komatiite
JP296	Pyroclastic
JP297	Pyroclastic
JP299	Pyroclastic
JP405	Wacke
JP480	Pyroclastic
JP487	Basalt

Table B-1

Appendix B Model Analysis (% by eye)

Sample	21a	21b	24	73	76	80	99	105	106	112	135	136	137	140	155	160	163	166	188
quartz	15	1	—	—	—	—	85	70	40	11	20	10	—	30	—	5	—	30	15
plagioclase	10	—	—	—	—	—	—	15	—	—	10	30	30	10	30	10	25	15	5
K-feldspar	—	—	—	—	—	5	—	—	—	—	—	—	—	—	—	—	5	—	—
amphibole	—	85	65	—	90	15	—	2	—	—	—	—	40	—	—	—	3	—	—
olivine	—	—	—	—	—	10	—	—	—	—	—	—	—	1	—	—	—	—	—
biotit	—	—	—	—	—	—	—	—	—	—	—	—	—	—	10	—	—	—	—
chlorite	60	10	35	—	10	55	—	3	—	—	50	10	30	5	50	5	52	35	50
sericite	8	—	—	—	—	—	—	—	30	—	17	—	—	39	—	58	—	—	—
epidote	—	3	—	5	—	—	—	—	—	—	—	—	—	—	—	—	—	3	—
calcite	4	1	—	23	—	10	5	5	20	80	—	5	—	10	5	15	5	—	25
opaques	3	—	5	12	—	5	10	5	5	4	3	—	—	—	2	7	15	5	5
serpentine	—	—	—	60	—	—	—	—	—	—	—	—	—	—	—	—	—	—	—
apatite	—	—	—	—	—	—	—	—	—	5	—	—	—	5	—	—	—	—	—
muscovite	—	—	—	—	—	—	—	—	—	—	—	2	—	—	3	—	—	—	—

Appendix B continued....

Sample	195	200	205	206	209	JP290	JP294	JP405	JP487
quartz	10	—	75	—	10	—	15	5	—
plagioclase	—	—	—	—	—	—	—	—	25
K-feldspar	—	—	—	—	—	25	—	—	—
amphibole	—	55	—	77	—	—	70	—	5
olivine	—	—	—	—	—	—	—	—	2
biotite	—	—	—	—	30	—	—	—	—
chlorite	—	30	2	10	15	15	5	—	35
sericite	—	—	—	—	—	5	10	—	—
epidote	—	—	—	—	—	—	—	—	3
calcite	15	5	15	10	30	29	—	95	30
opaques	—	10	8	8	5	1	—	—	2
serpentine	—	—	—	—	—	—	—	—	—
apatite	—	—	—	—	—	—	—	—	—
muscovite	—	—	—	—	—	—	—	—	—
clays	75	—	—	—	—	—	—	—	—

Appendix C Accuracy of XRF Determinations

1. Major Oxides

The accuracy of the X.R.F. analysis for major oxides was checked by running standards as unknowns and comparing them to recommended values (Abbey, 1975). The standards used were BCR-1, GSP-1, NIM-N, NIM-G, W-1 and SY-1. The following are the results for running standards.

	<u>BCR-1</u> (recommended)	<u>BCR-1</u> (unknown)	<u>W-1</u> (recommended)	<u>W-1</u> (unknown)
SiO ₂	54.85	54.98	52.72	52.38
TiO ₂	2.22	2.24	1.07	1.05
Al ₂ O ₃	13.68	13.44	14.87	14.65
Fe ₂ O ₃ (T)	13.52	13.83	11.11	10.98
MnO	0.19	0.20	0.17	0.17
MgO	3.49	3.20	6.63	6.59
CaO	6.98	7.12	10.98	11.01
Na ₂ O	3.29	2.92	2.15	2.49
K ₂ O	1.68	1.73	0.64	0.59
P ₂ O ₅	0.33	0.34	0.14	0.08

Errors are negligible (Similar results were obtained for the other standards).

2. Trace Element Analysis

As for the major oxides, the accuracy of the trace element analyses was checked by running standards as unknowns, and comparing them to recommended values (Abbey, 1975). For Rb, Sr, Y, Nb and Y, NIM-G, GSP-1, NIM-S, SY-1, W-1, BCR-1, NIM-L, NIM-D and MRG-1 were used as standards. The following are the

results for running standards.

	<u>GSP-1</u> (recommended)	<u>GSP-1</u> (unknown)	<u>BCR-1</u> (recommended)	<u>BCR-1</u> (unknown)
Rb	250	264	47	40
Sr	230	256	330	354
Y	32	25	46	51
NB	29	32	14	17
Zr				

Similar results were obtained for the other standards. For Cr, Co, Cu, Zn and As, standards GSP-1, W-1, BCR-1, AGV-1, NIM-G, NIM-L, JB-1, JG-1, NIM-D, SY-1, SY-2, SY-3, G-2 and MRG-1 were used. The following are the results for running standards NIM-D and W-1. (P.P.M.):

	<u>NIM-D</u> (recommended)	<u>NIM-D</u> (unknown)	<u>W-1</u> (recommended)	<u>W-1</u> (unknown)
Cr			120	108
Co	200	210	50	47
Cu	10	10	110	110
Zn	90	103	120	132
As		0	19	0

Similar results were obtained using the other standards. For Cr, standard JB-1 gave the following results:

	<u>JB-1</u> (recommended)	<u>JB-1</u> (unknown)
Cr	420	402

For Ni, standards NIM-P, BR, NIM-N, W-1, SY-1, BCR-1, NIM-D, MRG-1, GSP-1 and NIM-S were used. The following are the results obtained for running standards BR and NIM-N(P.P.M.):

	<u>BR</u> (recommend)	<u>BR</u> (unknown)	<u>NIM-N</u> (recommend)	<u>NIM-N</u> (unknown)
Ni	270	271.9	120	123.2

Error is insignificant. Similar results were obtained using the other standards.

Table D-1 Whole Rock Analyses (normalized to 100%)

sample	SiO ₂	TiO ₂	Al ₂ O ₃	Fe ₂ O ₃	MnO	MgO	CaO	Na ₂ O	K ₂ O	P ₂ O ₅	loss on ignition
21a	50.78	0.31	9.82	11.27	0.30	6.42	13.57	1.52	0.17	0.02	5.82
24	53.03	0.29	8.40	14.40	0.25	7.41	10.90	0.33	0.10	0.03	4.86
C31	47.95	0.28	8.39	12.65	0.20	13.40	10.81	0.60	0.13	0.04	5.55
73	31.93	0.08	2.67	9.33	0.21	12.38	2.97	0.17	0.03	0.04	40.13
76	57.84	0.14	4.51	7.91	0.25	7.49	16.46	0.34	0.06	0.02	4.97
80	44.69	0.79	13.68	15.47	0.35	5.22	10.35	0.96	0.56	0.02	7.90
106	50.38	0.87	15.08	7.88	0.26	3.46	6.28	3.30	1.87	0.34	10.28
108	49.58	0.72	12.75	14.15	0.28	6.19	10.75	1.44	0.15	0.02	3.95
112	36.08	0.04	1.53	6.32	0.68	6.08	20.22	0.36	0.28	0.02	28.40
135	67.85	0.46	15.41	3.53	0.08	1.52	2.39	1.75	3.11	0.06	3.85
136	69.68	0.51	15.26	4.94	0.13	1.60	3.62	2.96	2.06	0.03	4.21
137	49.58	1.43	14.83	9.92	0.15	4.85	7.40	2.68	1.98	0.35	6.81
140	64.95	0.42	17.31	4.80	0.14	1.69	3.38	2.09	2.34	0.02	2.86
150	67.53	0.53	14.99	3.90	0.20	1.16	2.70	0.53	3.58	0.02	4.85
155	73.98	0.30	9.46	5.13	0.21	1.80	3.31	1.26	0.76	0.02	3.78
160	69.77	0.31	13.56	3.47	0.06	0.87	3.50	1.70	2.30	0.02	4.43
161	72.63	0.17	13.25	2.04	0.05	3.64	0.95	1.30	3.04	0.02	2.91
166	60.01	0.61	15.83	9.89	0.18	3.31	4.33	2.41	1.24	0.02	2.17
188	50.84	0.76	16.21	8.63	0.17	4.30	5.93	4.03	1.17	0.29	7.67
200	74.77	0.08	3.18	9.08	0.22	4.81	5.71	0.21	0.12	0.03	1.78
205	81.83	0.04	1.88	8.67	0.27	1.79	0.57	0.19	0.05	0.05	4.67
206	52.47	0.16	5.31	20.32	0.45	6.67	10.95	0.41	0.34	0.02	2.90
209	49.44	0.65	16.96	8.41	0.15	3.71	7.04	3.93	3.00	0.30	6.42
185	72.0	0.19	14.5	1.63	0.03	0.31	1.41	3.91	2.34	0.05	2.00
188	65.1	0.80	15.0	3.59	10.08	1.41	5.02	4.17	1.52	0.09	2.50

Table D-2 Trace Element Analyses (R.P.M.)

Sample	Rb	Sr	Y	Nb	Zr	Cr	Co	Cu	Zn	As	Ni	S
21a	2	100	8	5	38	3498	50	27	83	0	854.4	0.03
24	0	2	0	4	18	3213	78	8	87	0	2098.2	0.03
PC31	2	34	0	4	28	2678	78	2.7	70	6.5	766.9	121
73	3	13	0	11	17	4283	75	5	62	15	213.0	0.05
76	0	0	0	4	16	3120	36	10	51	1	200.2	0.03
80	25	188	15	3	74	640	64	295	132	0	74.4	0.05
106	64	670	31	10	145	255	29	51	87	1	262.3	0.02
108	5	120	12	13	62	574	61	34	113	0	961.1	0.03
112	9	61	0	11	21	4622	27	7	44	263	27.6	0.03
135	111	208	8	18	138	47	14	8	49	7	29.4	0.02
136	78	3.04	10	15	156	54	13	8	75	0	203.1	0.03
137	135	4.07	15	14	169	244	36	112	97	0	139.6	0.04
140	54	144	1	4	50	41	31	6	44	33	219.5	0.04
150	154	61	0	11	36	4511	25	107	39	110	41.8	0.03
155	31	109	25	17	100	330	14	14	77	0	10.4	0.09
160	91	223	6	12	111	25	7	8	48	5	11.5	0.03
161	125	82	15	15	125	18	28	7	38	19	225.1	0.03
166	46	152	13	6	69	47	39	17	52	0	15.1	0.03
188	55	649	15	16	138	39	29	8	77	0	324.1	0.03
200	5	52	6	12	28	3439	43	6	55	0	1092.4	0.03
205	3	3	0	4	17	3436	53	9	41	245	1036.5	0.09
206	7	62	5	1	30	3360	124	9	86	15	18.2	0.03
209	122	759	17	12	127	52	24	46	79	0	119.9	0.06
JP485	90	250	10	—	160	460	5	10	34	4	16	—
JP488	70	80	10	—	40	6	16	60	32	7	58	—

Appendix E Equivalent Cation NormsTable E-1 Volcanics

NO.'S	21	24	73	76	80	106	108	*140	**166	188	200	206	***209
Qtz	6.5	14.7	2.6	20.4	2.6	5.3	6.0	32.9	22.3	2.2	53.1	10.9	
Alb	12.9	2.8	1.4	2.9	8.1	27.9	12.2	17.7	20.4	34.1	1.8	3.5	28.4
An	19.5	21.1	6.4	10.6	31.4	20.8	27.9	16.6	21.4	22.7	7.4	11.6	19.8
Or	1.0	0.6	0.2	0.4	3.3	11.1	0.9	13.8	7.3	6.9	0.7	2.0	17.7
Wo	19.9	13.7	3.4	29.6	8.3	3.4	10.6			2.0	8.7	17.8	5.5
En	10.3	6.6	2.2	18.6	3.4	1.9	4.9			1.1	4.3	6.5	2.9
Fs	9.1	6.9	0.9	9.2	5.0	1.4	5.5			0.8	4.1	11.7	2.4
Hp (EN)	5.7	11.9	28.6	0.1	9.6	6.7	10.5	4.2	8.2	9.6	7.6	10.1	
Fs	5.1	12.5	10.9	0.03	14.2	4.8	11.7	2.7	10.4	6.9	7.2	18.3	
Fo													4.4
Fa													4.1
ilm	0.6	0.6	0.2	0.3	1.5	1.7	1.4	0.8	1.2	1.4	0.2	0.3	1.2
Apt.	0.1	0.1	0.1	0.1	0.1	0.8	0.1	0.1	0.1	0.7	0.1	0.1	0.7
Mt.	2.6	2.6	2.3	2.4	3.3	3.4	3.2	3.2	3.0	3.3	2.3	2.4	3.1

* Corundum 5.2

** Corundum 2.7

*** Nephelene 2.6

Key for Appendix E

Qtz - Quartz	Fs - Ferrosilite	Apt - Apatite
Or - Orthoclase	Fo - Forsterite	Hp - Hypersthene
Alb - Albite	Fa - Fayalite	Wo - Wollastonite
An - Anorthite	Mt - Magnetite	
En - Enstatite	Ilm - Ilmanite	

Table E-2 Pyroclastics

NO.'S	135	136	150	160	* 161
Qtz	38.4	28.3	43.8	42.0	46.0
Alb	14.8	25.0	4.5	14.4	11.0
An	11.5	17.8	13.3	17.2	4.6
Or	18.4	12.2	19.7	13.6	18.0
Wo					
En					
Fs					
Hp(EN)	3.8	4.0	2.9	2.1	9.0
Fs	0.4	2.6	0.9	0.8	0.0
Fo					
Fa					
ilm	0.9	1.0	1.0	0.6	0.3
Apt.	0.1	0.1	0.1	0.1	0.1
Mgt.	2.8	2.9	2.9	2.6	0.7
Corundum	5.0	1.7	5.6	2.0	6.1

* Hematite 1.2

References

- Abbey, S., 1975, Studies in standard samples of silicate rocks and minerals. Part 4: 1974 edition of usable values. Geol. Surv. Canada, Paper
- Arndt, N.T., Naldrett, A.J.N. and Pyke, D.R., 1977, Komatiitic and iron-rich tholeiitic lavas of Munro Township, Northeast Ontario. Jour. Petrology, Vol.
- Arth, J.G., Arndt, N.T. and Naldrett, A.J., 1977, Genesis of Archean Komatiites from Munro Township, Ontario: Trace-element evidence. Geology, Vol. 5, p. 590-594.
- Brooks, C. and Hart, S.R., 1972, An extrusive basaltic komatiite from a Canadian Archean metavolcanic belt. Can. J. Earth Sci., Vol. 9, p. 1250-1253.
- Carmichael, I.S.E., Turner, F.J. and Verkoogen, J., 1974, Igneous Petrology. McGraw-Hill, New York, 759 p.
- Erlank, J.A., 1968, The terrestrial abundance relationship between potassium and rubidium, in Origin and Distribution of the Elements. Ahrens, L.H. (Ed.), International Series of Monographs in Earth Sciences, Pergamon Press, Vol. 30, p. 871-888.
- Ferguson, S.A., 1966, Geology of Dome Township, Ontario Dept. of Mines Geological Report 45, 98p.
- Fiske, R.S., 1963, Subaqueous pyroclastic flows in the Ohnapocosh Formation, Washington. Geol. Soc. Amer. Bull. Vol. 74, p. 391-406.
- Goodwin, A.M., 1977, Archean basin-craton complexes and the growth of Precambrian shields. Can. Journ. Earth Sci., Vol. 14, No. 12, p. 2737-2759.

- Horwood, H.C., 1940, Geology and Mineral Deposits of the Red Lake Area. 49th Annual Report of the Ont. Dept. Mines. Vol. XLIX, Part II, 231 p.
- Hyndman, D.W., 1972, Petrology of Igneous and Metamorphic Rocks. McGraw-Hill Book Company, 533 p.
- Irving, T.N. and Baragar, 1971, A guide to the chemical classification of the common volcanic rocks. Can. Jour. Earth Sci., Vol. 8, p. 523-548.
- Jenson, L.S., 1976, A new cation plot for classifying subalkalic volcanic rocks. Ministry of Natural Resources, Misc. Paper 66, 22p.
- Kita, J.H., 1978, Geology and genesis of the east shore of Hoyles Bay. Bateman and McDonough Townships, Red Lake Area Ontario. Bachelor Thesis, Dept. of Geological Engineering, University of Toronto, 57 p.
- Longstaff, F.J., 1977; The oxygen isotope and elemental geochemistry of Archean rocks from northern Ontario. Ph.D. Thesis, McMaster University.
- Mason, B., 1952, Principles of geochemistry, John Wiley & Sons Inc.
- Naldrett, A.J., and Mason, G.D., 1968, Contrasting Archean ultramafic igneous bodies in Dundonald and Clergue Townships, Ontario; Can. Jour. Earth Sci., Vol. 5, p 111-143.
- Naldrett, A.J. and Cabri, L.J., 1976, Ultramafic and related mafic rocks: their classification and genesis with special reference to the concentration of nickel sulfides and platinum-group elements. Econ. Geol., Vol. 71 p. 1131-1158.
- Pearce, J.A., and Cann. J.R., 1973, Tectonic setting of basic volcanic rocks determined using trace element analyses. Earth and Planetary Science Letters., North-Holland Publishing Company, p. 290-300.
- Pirie, J., 1977, Bateman-Balmer Townships area, District of Kenora, Patricia

Portion. No. 3, in Summary of field work, 1977. Ont. Geol. Survey. Misc. Paper 75, Ministry of Nat. Resources.

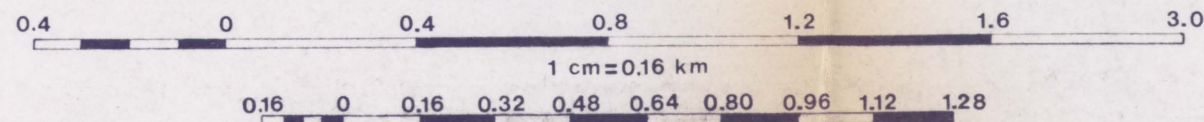
- Pirsson, L.V., 1915, The microscopical characters of volcanic tuffs - A study for students. Amer. Jour. Sci., Vol. 40, p. 191-211.
- Pyke, D.R., Naldrett, A.J. and Eckstrand, O.R., Archean ultramafic flows in Munro Township, Ontario. Geol. Soc. Amer. Bull. Vol. 84, p. 955-978.
- Rankama, K. and Sahama, G.; 1950, Geochemistry. University of Chicago Press.
- Schnetzler, C.C. and Philpotts, J.A., 1968, Partition coefficients of rare earth elements and barium between igneous matrix material and rock forming mineral phenocrysts in Origin and Distribution of the Elements. Ahrens, L.H. (Ed.), International Series of Monographs in Earth Sciences, Vol. 30, p. 929-938.
- Shaw, D.M., 1970, A review of K-Rb fractionation trends by covariance analysis. Geochimica et Cosmochimica Acta, Vol. 32, p. 573-601.
- Shelley, D., 1975, Manual of Optical Mineralogy. Elsevier Scientific Publishing Co.
- Williams, H., Turner, F.J. and Gilbert, C.M., 1954, Petrography, An introduction to the study of rocks in thin sections: W.H. Freeman and Co.
- Wilson, H.D.B., Andrews, P., Monham, R.L., and Ramlal, K., 1965, Archean volcanism in the Canadian Shield. Can. Jour. Earth Sci., Vol. 2, p. 161-175.



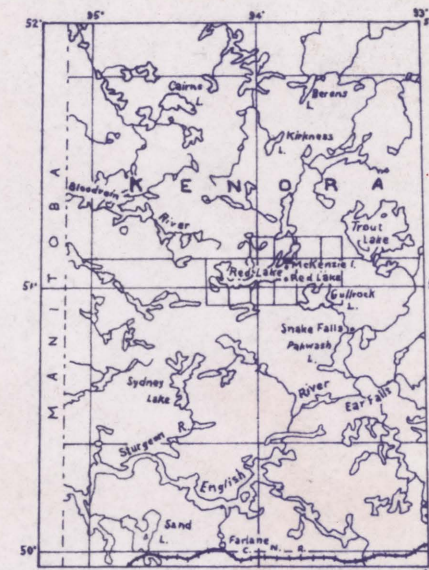
THESIS AREA

Scale; 1 cm. to 0.16 km.

1 in = 0.4 km



LOCATION MAP



Scale, 1 cm to 31.7 km

LEGEND

PRECAMBRIAN

INTRUSIVE ROCKS

- 11 11 Porphyritic metagabbro
- 10 10 Quartz porphyry
- 9 9 Quartz diorite (border phase of McKenzie Island stock)
- 8 8 Serpentinite

-intrusive contact-

METASEDIMENTARY ROCKS

- 7 7 Alternating bands of iron formation, slate, chert, wacke

CHEMICAL METASEDIMENTS

- 6 6 Lean iron formation
- 5 5 Limestone

CLASTIC METASEDIMENTS

- 4a 4a Wacke
- 4b 4b Mudstone
- 4c 4c Slate

METAVOLCANIC ROCKS

FELSIC METAVOLCANICS

- 3a 3a Volcanic breccia
- 3b 3b Lapilli-tuff
- 3c 3c Tuff

MAFIC METAVOLCANICS

- 2 2 Basaltic komatiites
- 1a 1a Tholeiitic basalt
- 1b 1b Altered tholeiitic basalt or calc-alkali andesite

SYMBOLS

- ○ ○ ○ Variolitic metabasalt
- ○ ○ ○ Pillowed metabasalt
- ○ ○ ○ Pillow breccia
- ○ ○ ○ Carbonatized rock
- Glacial striae
- Small rock outcrop
- Boundary of rock outcrop
- Geological boundary, defined
- Geological boundary, approximate or assumed
- Strike and dip, direction of top unknown
- Strike and vertical dip, direction of top unknown
- Direction (arrow) in which inclined beds face as indicated by graded bedding
- Direction in which lava flows face as indicated by shape of pillows
- Strike and dip of schistosity
- Strike of schistosity, dip unknown
- Drill hole, vertical, inclined

